DANMARKS OG GRØNLANDS GEOLOGISKE UNDERSØGELSE RAPPORT 2010/58

Annual workshop on the geology of southern West Greenland related to field work: abstract volume II

Compiled and edited by Thomas F. Kokfelt & Jochen Kolb

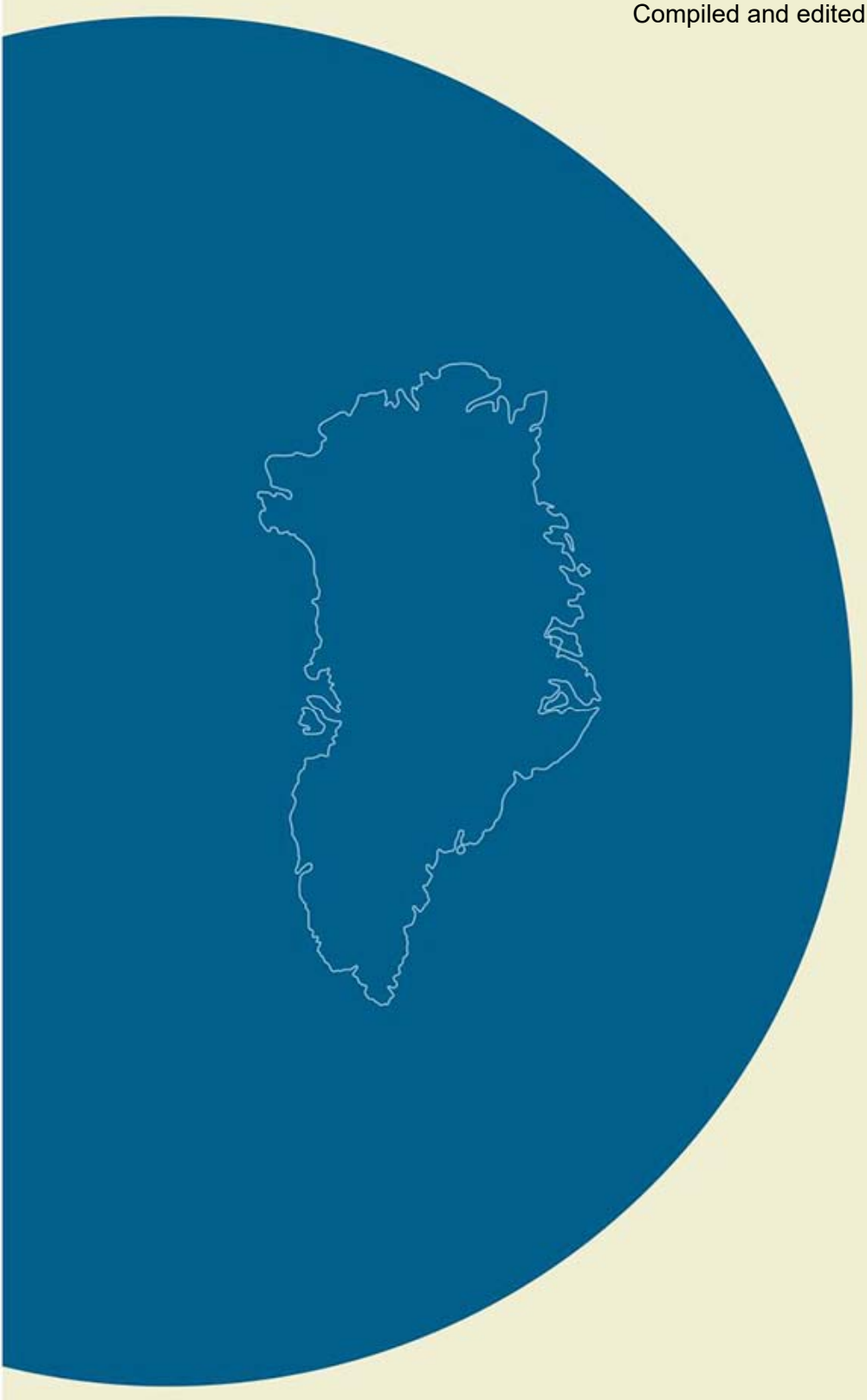

GEOLOGICAL SURVEY OF DENMARK AND GREENLAND
MINISTRY OF CLIMATE AND ENERGY

GEUS

DANMARKS OG GRØNLANDS GEOLOGISKE UNDERSØGELSE RAPPORT 2010/58

Annual workshop on the geology of southern West Greenland related to field work: abstract volume II

Compiled and edited by Thomas F. Kokfelt & Jochen Kolb

GEOLOGICAL SURVEY OF DENMARK AND GREENLAND
MINISTRY OF CLIMATE AND ENERGY

GEUS

Table of Contents

Annual workshop on the geology of southern West Greenland related to field work: abstract volume II

Foreword

It is a long tradition that GEUS organises a workshop related to its field activities in Greenland, bringing together geologists from GEUS and all the external collaborators. The basic idea of these workshops is to present and discuss data collected during field work and later laboratory work at home. The focus is aimed to be on the discussions. At the same time, field activities for the upcoming field season are discussed and organised, and for the first time this year, a security course for the external collaborators is organised.

In this volume, abstracts are collected that cover topics on field work in 2009 and topics that cover areas of future interest related to the field work plans in southern West Greenland. The abstracts reflect the work that has been done since 2008 in various projects co-financed by the Bureau of Minerals and Petroleum (BMP) and the Geological Survey of Denmark and Greenland (GEUS), namely (1) Homogenisation and conceptual modernisation of geological maps of the region at scale 1:100,000; (2) Integrative data analysis for characterisation and favourability of economic metals, southern West Greenland, 61°30'–64°; (3) Structurally controlled hydrothermal alteration and mineralisation on a regional scale and detailed studies of selected greenstone belts, southern West Greenland, 61°30'–64°; and (4) Economic potential of gabbro-anorthosites in the Fiskenæsset region. These projects run from 2008–2010 and cover the area between 61°30'–64° in southern West Greenland. This is the second abstract volume and the second workshop in this 3-year project.

The program is given on the following page and the abstracts in this volume occur in alphabetical order of the principal author. This abstract volume is aimed at giving basic information about the presentations and as a reminder back home.

We wish you all a pleasant and informative workshop at GEUS.

God fornøjelse,

Jochen and Thomas

Thursday, 17th June Room: Theodor Sorgenfrei

Time	Session	Authors	Title	Chairman
09:00 - 09:30			Welcome	
09:30 - 09:50	Geology of the Fiskenæsset & Grædefjord areas	Keulen, Næraa, Kokfelt, Schumacher, Scherstén	Zircon record of the igneous and metamorphic history of anorthosite from Fiskenæsset complex, southern West Greenland	Kolb
09:50 - 10:10		Appel, Dahl, Kalvig, Polat	PGE discoveries in the ~2970 Ma Fiskenæsset anorthosite comples, West Greenland	
10:10 - 10:30		Kisters, Bergen, Kokfelt, Kolb	Structural geology of the Grædefjord, southern West Greenland	
10:30 - 10:50		Coffee break		
10:50 - 11:10	Supracrustal rocks and their metamorphic & metasomatic history	Keulen, Schumacher, van Hinsberg, Szilas, Windley, Kokfelt	The Bjørnesund anorthosite-greenstone belt - linking the Fiskenæsset complex to the Ravn Storø metavolcanic belt	Kokfelt
11:10 - 11:30		Schumacher, Stamper, Sherwood, Keulen, Piazolo	Pressure and temperature constraints on metamorphism of and the P-T trajectory for altered volcanic rocks from Qilanngarssuit island, east of Qarajat Iluat Fjord and Ikatoq Nuna	
11:30 - 11:50		Szilas	Supracrustal rocks of the Tartôq Group, south West Greenland	
11:50 - 12:10		Bergen, Kolb, Konnerup-Madsen	Characteristics of the hydrothermal alteration and mineralisation in the Kangiata Nuna and Sermilik region	
12:10 - 13:00		Lunch		
13:00 - 13:20		Nilsson· Söderlund, Ernst, Hamilton, Scherstén, Armitage	U-Pb ages of mafic intrusions in the North Atlantic Craton, and implications for a palaeoreconstruction	
	Poster session	Kokfelt, Keulen, Heijboer, Næraa, Scherstén	Thematic age distribution maps of the Archaean basement, southern West Greenland	
		Kolb, Schlatter, Stensgaard, Dziggel	Controls on Quartz ± Gold Vein Formation and Hydrothermal Alteration in the Færingehavn and Tasiusarsuaq Terranes, southern West Greenland	
13:20 - 14:00		Lewerentz, Keulen, Kokfelt, Scherstén	On the origin of baddeleyite in zircon in quartz-saturated rocks from the Sermilik and Bjørnesund blocks, southern West Greenland	
		Næraa, Scherstén, Kokfelt	Field observations, whole rock chemistry and combined zircon U/Pb/Hf/O isotope analyses from the Ilivertalik Augen Granite, southern West Greenland: Evidences for an igneous granite - charnockite relationship	
14:00 - 14:20	Digital field capturing & PDA	Schlatter, Larsen, Stensgaard	Digital field data capture in Greenland: GanFeld news	
14:20 - 16:00		Schlatter	Demonstration of the PDA	
16:00 - 18:00		Open discussion		
19:00 - END		Dinner	Restaurant MOGOGO (Borgergade 134)	

PGE discoveries in the ~2970 Ma Fiskenæsset anorthosite complex, West Greenland

Peter W. U. Appel, Ole Dahl, Per Kalvig & Ali Polat

A re-evaluation project on the PGE potential of the Fiskenaesset anorthosite complex has been carried out in 2008 and 2009; the project was a joint project between Bureau of Minerals and Petroleum (BMP) and GEUS.

The Fiskenaesset anorthosite complex was emplaced ~2970 Ma ago as multiple sills of magma and crystal mush into oceanic crust (tholeiitic basalts and gabbros), forming an association of ~550 m thick anorthosite, leucogabbro, gabbro and peridotite layers. The complex has a present strike length of ~200 km. It has been partly broken up during multiple deformations, and suffered amphibolite- to granulite facies metamorphism. Chromite-rich bands are common throughout the complex; sulphide-rich layers are generally rare.

The first traces of platinum group elements (PGE) were discovered in a chromitite banded bronzitite in the late 1960'ies and prompted several exploration campaigns in the subsequent decade, but without encouraging results. During a campaign undertaken by GEUS in 1991 new PGE occurrences were discovered, but due to those days low price level of PGE the results did not attract further attention.

During the field season 2009 detailed work was carried out on northern Qeqertarssuatsiaq Island and nearby Itise, comprising detailed geological mapping, and chip- and channel sampling. Eight profiles were sampled, revealing PGE's in small but significant amounts throughout the ultrabasic rocks with a significant enrichment in a ~5 m thick reef, named Ghisler Reef, grading 690 ppb combined Pt, Pd and Au over 5 m with best values within the Reef of 2 ppm Pt, Pd and Au with 20 ppb Rh over 1 m. The PGE-bearing unit can be traced with intervals for ~5 km and an exposed thickness up to 50 m. Limited sampling of a few chromitite layers revealed a up to 106 ppb Pd and 370 ppb Pt.

Ghisler Reef displays an unusual geochemical signature with near perfect correlation of Pt, Pd, Au and Cu with Bi. This geochemical signature is in good accordance with the observed presence of PGE-Bi bearing minerals such as froodite $PdBi_2$, sobolevskite (Pd, Pt)Bi, insizwaite $PtBi_2$, maslovite PtTeBi, michenerite (Pd, Pt)TeBi, keithconnite Pd_{1-x}(Te, Bi), unnamed $Cu_3Pt_3Bi_4S_{10}$, electrum AuAg, native Ag, parkerite $Ni_3Bi_2S_2$ and native Bi. Ghisler Reef has low contents of sulphur.

The association of PGE with bismuth is seen in deposits such as Sudbury, Great Dyke and Monchegorsk intrusion on Kola Peninsula.

The discovery of ultrabasic rocks highly enriched in PGE has opened up parts of the 200 km long Fiskenaesset anorthosite complex for finding economic PGE deposits.

Investigations were also conducted on the complex' rock units in the Sinarsuk area near the Inland Ice, as well on selected ultrabasics not forming part of the complex, but no encouraging geochemical data have been returned.

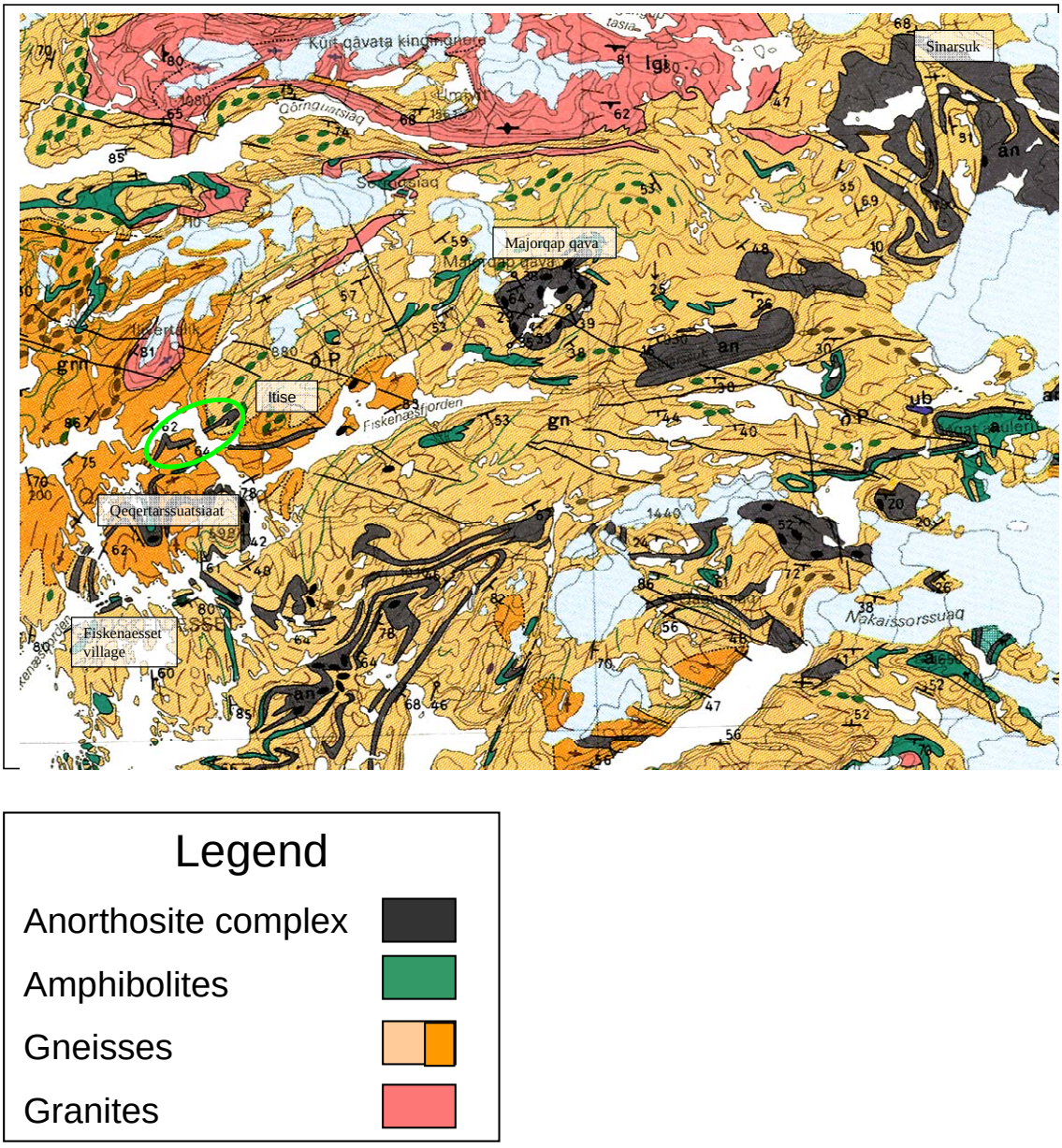

Figure 1. *Index map showing distribution of the anorthosite complex and target areas; the green circle indicates the Qeqertarssuatsiaat area and the Itise area. Legend equivalent to the GGU 1:500 000 map.*

Reference

Appel, P. W. U., Dahl, O., Kalvig, P. & Polat, A. 2010. Discovery of new PGE mineralization in the Precambrian Fiskenæsset anorthosite complex, West Greenland. Danmarks og Grønlands Geologiske Undersøgelse Rapport, **2010/29**, 42 pp. CD enclosed

Characteristics of the hydrothermal alteration and mineralisation in the Kangiata Nunaa and Sermilik region

Anders Bergen, Jochen Kolb & Jens Konnerup-Madsen

During the 2008 and 2009 GEUS summer campaigns in southern West Greenland, south of Nuuk, samples for studies intended for investigations of potential mineralisation in the eastern - (Kangiata Nunaa region) and southern part (Sermilik region) of the Archaean Tasiusarsuaq terrane where collected.

Samples of quartz veins and associated hydrothermal alteration zones, and from nearby host-rocks from the Kangiata Nunaa and Sermilik regions have been studied in order to characterise the hydrothermal alteration and mineralisation within the two regions.

In the Kangiata Nunaa region, the TTG gneisses and amphibolites contain a hydrothermal alteration assemblage comprising Bt-Qtz-Hbl-Grt and minor amounts of Fe-Ti oxides, Ccp and Py. Whole rock analysis from the Kangiata Nunaa region reports Au-contents of up to 20 ppb from the hydrothermal alteration zones and associated quartz veins.

In the Sermilik region, the hydrothermal alteration assemblage of meta-sedimentary host-rocks consists of Bt-Qtz-Grt-Sil-Kfs and minor amounts of Fe-Ti oxides, Py and Rt. Whole rock analysis reports a Au-content for one quartz vein sample of 6370 ppb, whereas other hydrothermal alteration zones and quartz vein samples have Au values between 2 and 30 ppb.

Samples have been studied to establish the paragenetic relationships in the individual hydrothermal alteration zones within each region in order to determine and divide the mineral assemblages into pre-, syn- and post-alteration stages. The mineral paragenesis of the pre-alteration stage consists of Pl-Qtz-Kfs-Hbl-Grt-Bt-Cpx, a syn-alteration stage of Bt-Qtz-Hbl-Grt and a post-alteration stage mainly consisting of Chl-Ep-Ms-Zo.

The EMP analytical data of hornblende shows an apparent trend of increasing Fe-content and decreasing Mg-content, and decreasing Ca-content and a slight increase in Mg-content from least altered samples into the proximal hydrothermal alteration zone. The whole rock Fe-Mg content in amphibolites and gneisses shows a trend of increasing Fe and decreasing Mg towards the proximal hydrothermal alteration zone.

The main difference between the Kangiata Nunaa and Sermilik regions, is the stability of an aluminous phase and K-feldspar in the Sermilik region, which is absent in the Kangiata Nunaa region. The Kangiata Nunaa region mineral assemblage also bears indications of a post-alteration metamorphic greenschist facies overprint, indicated by the presence of a Chl-Ep-Ms-Zo assemblage. Zosite is observed crosscutting the assemblage of the hydrothermal alteration. Biotite is chloritised and plagioclase altered to sericite.

Based on the paragenetic relationships, temperature and where possible the pressure determinations of the hydrothermal alteration conditions for the two regions have been calculated. These calculations indicate PT conditions corresponding to the amphibolite facies at around 3.5-4 kbars and 650 °C for the syn-alteration stage.

The samples of the low-Au region of Kangiata Nunaa and the Au mineralised region of Sermilik show similar mineralogical and geochemical compositions and PT conditions. The difference between the regions is the absence of an aluminous phase and K-feldspar in the Kangiata Nunaa region. This region also bears indications of a late post-alteration retro-

gressive greenschist facies metamorphic overprint, which is not seen in the host-rocks of the Sermilik region and could possibly be responsible for remobilising the gold from the hydrothermal alteration zones and quartz veins in the Kangiata Nunaa region.

The Bjørnesund anorthosite-greenstone belt – linking the Fiskenæsset complex to the Ravn Storø metavolcanic belt

Nynke Keulen[1], John C. Schumacher[2], Vincent van Hinsberg[3], Kristoffer Szilas[1], Brian Windley[4] & Thomas F. Kokfelt[1]

1) Geological Survey of Denmark and Greenland, Øster Voldgade 10, DK-1350 Copenhagen K, Denmark. E-mail: ntk@geus.dk
2) Department of Earth Sciences, University of Bristol, Bristol BS8 1RJ, UK.
3) Department of Earth and Planetary Sciences, McGill Univ., Montreal, Canada
4) Department of Geology, University of Leicester, Leicester LE1 7RH, UK.

Objective

The Bjørnesund anorthosite-greenstone belt is located on both sides of Bjørnesund (fjord) just south of 63ºN in southern West Greenland (Fig. 1). It consists of amphibolite and anorthosite, ultramafic lenses, a quartz-dioritic gneiss, and is intruded by granites and granodiorites, and surrounded by granodioritic to tonalitic grey orthogneisses (Fig. 1). The Bjørnesund belt is an amphibolite-leucogabbro-diorite association interpreted as an amphibolite-facies grade equivalent of a greenstone belt.

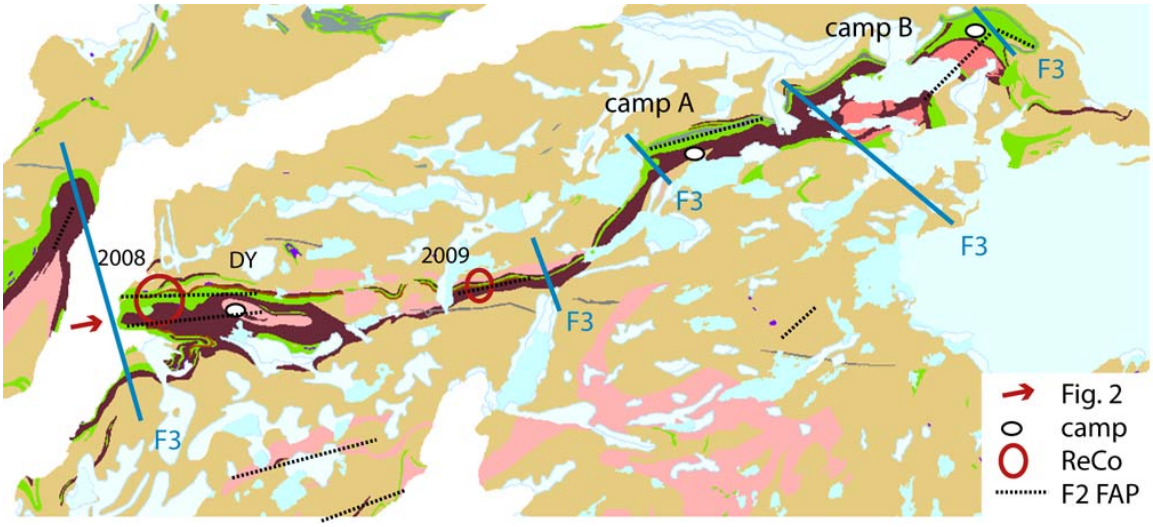

Figure 1. *Part of the 100K Bjørnesund map sheet (Escher 1976), showing the amphibolite (green)-diorite (dark red)-anorthosite (grey)-complex, the locations of the camps and the ReCo stops. DY = Denis Schlatter and Yong Chen. Axial plane traces of F3 and locally F2 folds (FAP) are shown.*

The contact relations between the intrusive Fiskenæsset complex and the amphibolites in the Fiskenæsset area can only be studied in a few places (e.g. Walton 1973; Escher & Myers 1975). The anorthosites in the Bjørnesund anorthosite-greenstone belt are considered to be part of the Fiskenæsset complex (e.g. Myers 1985). Where best preserved, the amphibolites contain many primary lithologies and volcanic structures such as lithic tuffs,

which are similar to those in the Ravn Storø metavolcanic belt (Ikkattup Nunaa belt) (conf. field observations 2008 and 2009 on the Bjørnesund anorthosite-greenstone belt and on Ikkattup Nunaa; see e.g. Fig. 1, 2). Therefore, the Bjørnesund belt provides an ideal opportunity to understand the contact relationships between the Ravn Storø metavolcanic belt and the Fiskenæsset complex. Furthermore, the Bjørnesund anorthosite-greenstone belt is the only area in southern West Greenland where amphibolites occur in contact with diorite.

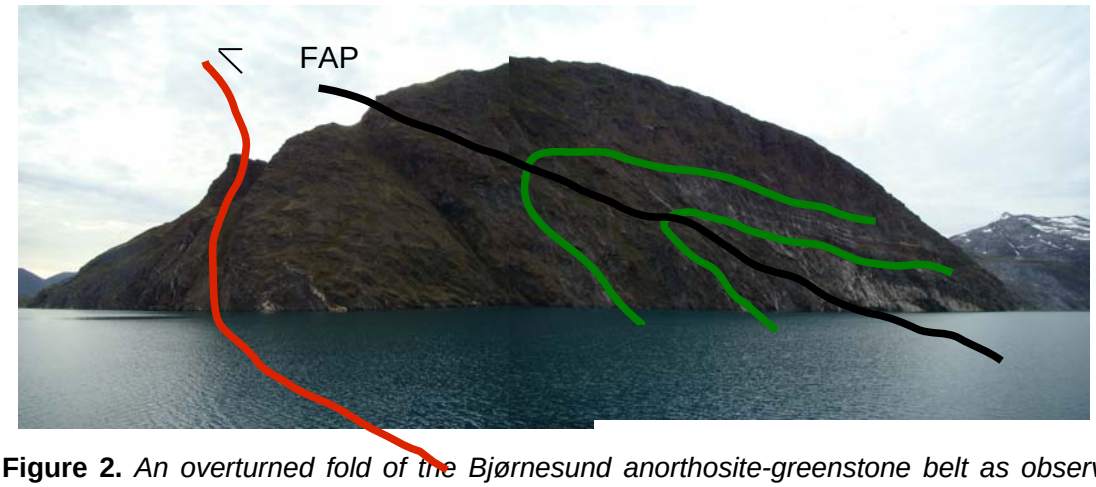

Figure 2. *An overturned fold of the Bjørnesund anorthosite-greenstone belt as observed from Bjørnesund looking to the east. FAP indicates the F2 fold axial plane. See Figure 1 for locality.*

Geology

The amphibolite layers are locally (e.g. near camp A at 62.95º N, 49.76º W; see Fig. 1) very intensely deformed. However, further east (at camp B at 62.99ºN, 49.54ºW; see Fig. 1) the amphibolites are almost undeformed, and here the preliminary observations in 2008 can be confirmed. The amphibolites contain similar lithostratigraphy, volcanic structures and rocks as in the Ravn Storø metavolcanic belt (Ikkattup Nunaa belt). For example, layered leuco-amphibolites, coarse homogeneous mela-amphibolites, lithic tuff fragments in leuco-amphibolite, and very diagnostic aplite dykes containing garnets with leucocratic haloes. In the Ravn Storø metavolcanic belt the undeformed and little deformed equivalents of the upper part of the Bjørnesund layered amphibolites contain pillow lavas, interlayered leuco-amphibolites and mela-amphibolites, distinctive lithic tuffs, and aplitic layers and dykes containing garnets with leucocratic haloes.

In the Bjørnesund area the assemblage hornblende and plagioclase ± quartz ± minor biotite is dominant for the amphibolites, but locally these rocks may contain garnet, cummingtonite or orthoamphibole. The presence of garnet is indicative of a bulk composition slightly enriched in FeO and lower in CaO, while the presence of cummingtonite and orthoamphibole suggests bulk compositions that are either richer in MgO or lower in CaO. Amphibolites that contain cummingtonite or anthophyllite are also typical of amphibolite- to upper amphibolite-facies conditions. Amphibolites in the Ravn Storø belt have slightly lower metamorphic grades (see Schumacher et al., this volume).

The amphibolites were intruded by a sheet, which mainly consists of leucogabbro (locally cumulate), gabbro and anorthosite locally with chromitite layers. Way-up criteria (An-Hbl graded layers) indicate right-way-up in the south of the sheet but inverted in the north. This sheet will here be referred to by its name on the original 1:100 000 map: anorthosite.

The anorthosite is folded into an isoclinal synform (F1) that has also affected the diorite and amphibolite (Fig. 3).

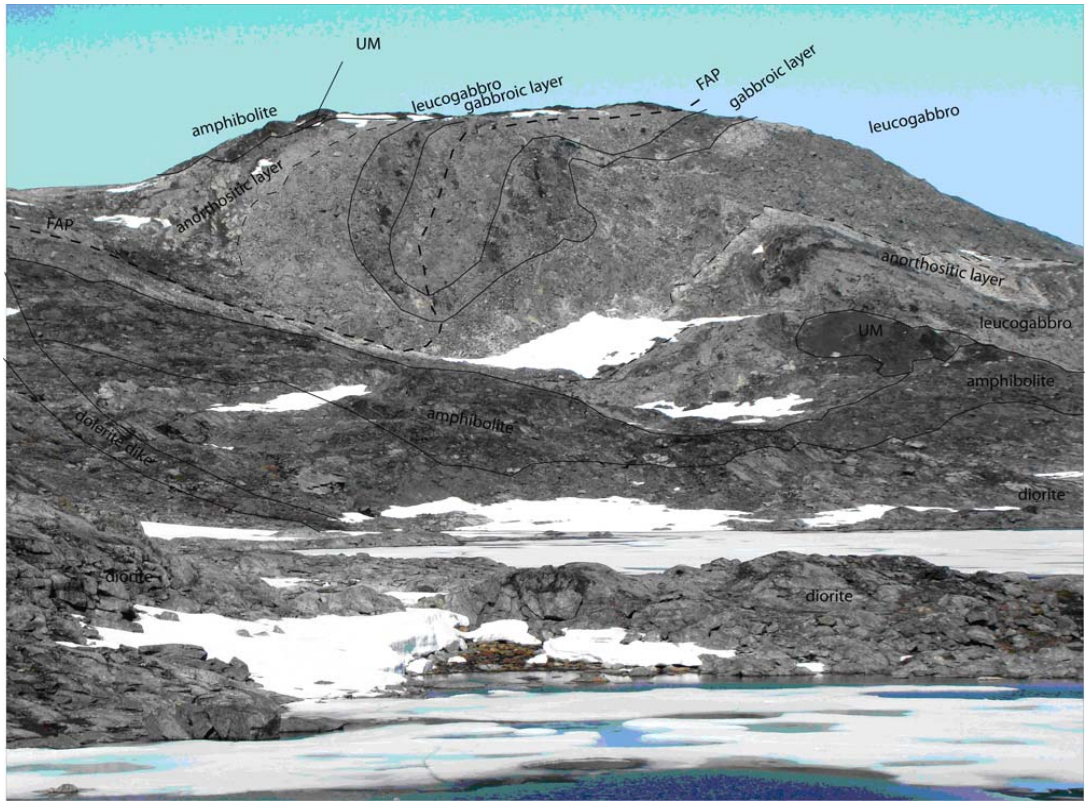

Figure 3. *Isoclinally folded (F1+F2) leucogabbro, gabbro, anorthosite and amphibolite as seen near camp A.*

Large lenses of ultramafic rocks occur locally along the contact of the amphibolites and the anorthosites. The central part of the ultramafic lenses is formed by a nearly pure clinopyroxene body. The ultramafic rocks show variable degrees of post-emplacement (?) hydration and commonly contain anthophyllite along with relict diopside and possible orthopyroxene and olivine. Locally, ca. 1 metre-thick metasomatic reaction zones (anthophyllite ± green pargasite ± green spinel ± sapphirine ± phlogopite) have formed at the contacts particularly in the presence of quartzo-feldspathic pegmatite. In these metasomatic zones pale-brown anthophyllite typically forms rosettes. At one locality, a pegmatite associated with the metasomatism contains iridescent orthoamphibole (up to 10 cm long) and subhedral cordierite up to 12 by >> 30 cm. At one location along the margin of this pegmatite, there is pink corundum in plagioclase. Chromite forms layers in the amphibolite and anorthosite just above and below the ultramafic rocks.

The ultramafic bodies form σ-clasts in intensively sheared anorthosite. The anorthosites are mostly sheared to finely banded anorthosite mylonite; the shearing, facilitated by the presence of minor biotite in the anorthosite (map-unit), is associated with F2 folds, the axial planes of which strike NS, as seen east of camp B.

The diorite is a medium- to fine-grained, homogeneous gneiss that consists of predominantly feldspar, minor quartz and biotite, and rare hornblende. Amphibolitic dykes transect the foliation at a low angle. A quartz diorite sample collected by Denis Schlatter in the western part of the Bjørnesund belt (Fig. 1) yielded a zircon U-Pb age of 2.919 ± 2 Ga (MSWD = 0.97, n/N = 61/64).

The amphibolites and anorthosites above were intruded by the protoliths of granodioritic to tonalitic gneisses. The gneiss contains a variety of felsic layers and locally changes towards a Bt-granite composition. The gneiss shows relatively complex zircon age pattern with a 2.87-2.89 Ga protoliths age peak (as identified by zircons with high Th/U ratio), locally overprinted by a ~2.70 Ga event. The gneiss was affected by the F2 folding. Late granites intruded the amphibolite-anorthosite belt; the largest is the Nukagpiarssuaq Granite that intruded an F2 fold core; it has a poorly constrained intrusion peak age of ~2.84 Ga and a large population of low Th/U ratio zircons between 2.75 and 2.70 Ga. Two further granite samples with the same protolith age bracket and the same structural setting were collected by Denis Schlatter in the western part of the Bjørnesund anorthosite-greenstone belt. The granites from the western part of the belt show very limited evidence for a ~2.70 Ga metamorphic overprinting in their zircon age distribution. A mild overprint of a later folding phase, F3, trending NNW-SSE has slightly bent the regional foliation, causing the staircase-like appearance of the Bjørnesund anorthosite-greenstone belt on the geological map.

Interpretation

The observed stratigraphy of the anorthosite is distinctly similar to that reported from the Fiskenæsset complex (e.g. Windley *et al.* 1973; Myers 1985). Compared with stratigraphy of the Fiskenæsset Complex (Myers 1985), the gabbro-leucogabbro-anorthosite units are present together with the ultramafic lenses and their sapphirine-bearing metasomatic zones, and with the bordering metavolcanic amphibolites, but the Upper Gabbroic Unit (Myers 1985, p. 14) is absent. The observed distribution of rocks outlines a synclinal structure in the Bjørnesund area, which is comparable with that of the Fiskenæsset complex farther north. The orientations of F2 and F3 fold axial planes are concordant with those of the Fiskenæsset complex (Myers 1985).

In addition to the lithostratigraphy suggesting a connection between the Ravn Storø metavolcanic belt and the amphibolites of the Bjørnesund belt, but also there is a structural connection, which is demonstrated by a cross-section between the two areas (Fig. 4). The amphibolites in the two areas are parts of the same sheet of extrusive rocks that were folded and thrust (probably with only minor displacement) during the regional D2 deformation event.

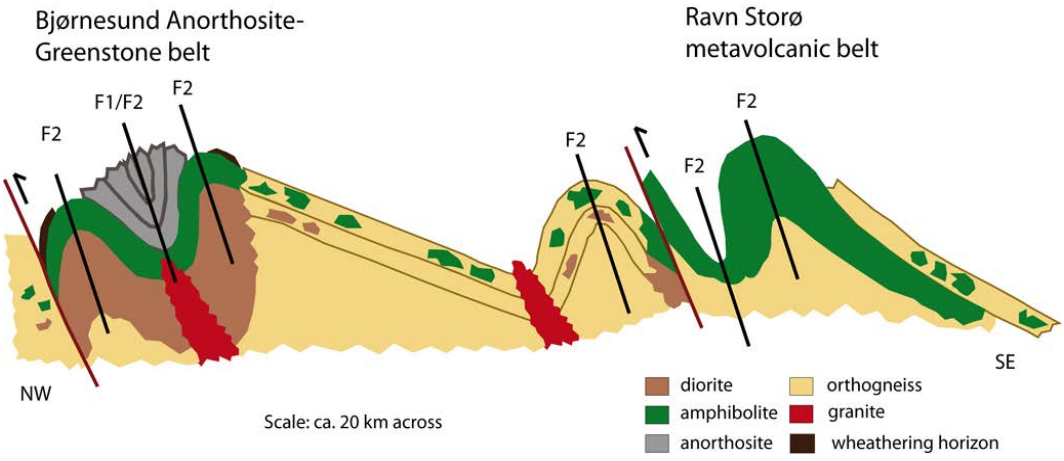

Figure 4. *Schematic cross-section through the Bjørnesund Anorthosite-Greenstone Belt and the Ravn Storø metavolcanic belt.*

References

Escher, J. 1976: Geologisk Kort over Grønland, 62V1 Nord, Bjørnesund 1:100,000.

Escher, J. & Myers, J.S. 1975: New evidence concerning the original relationships of early volcanics and anorthosites in the Fiskenæsset region, southern West Greenland. Grønlands Geologiske Undersøgelse Rapport **75**, 72-76.

Myers, J.S. 1985: Stratigraphy and structure of the Fiskenæsset Complex, southern West Greenland. Grønlands Geologiske Undersøgelse Bull. **150**, 72 pp.

Walton, B.J. (1973) The structure and stratigraphy of the anorthosite complex in the area north of Bjørnesund, near Fiskenæsset. Rapp. Grønlands Geologiske Undersøgelse, **51**, 60-64.

Windley, B.F., Herd, R.K. & Bowden, A.A. 1973: The Fiskenæsset Complex, West Greenland, Part 1: A preliminary study of the stratigraphy, petrology, and whole rock chemistry from Qeqertarssuatsiaq. Grønlands Geologiske Undersøgelse Bull. **106**, 80pp.

Zircon record of the igneous and metamorphic history of anorthosite from the Fiskenæsset complex, southern West Greenland

Nynke Keulen[1], Tomas Næraa[1], Thomas F. Kokfelt[1], John C. Schumacher[2] & Anders Scherstén[3]

1) *Geological Survey of Denmark and Greenland, Øster Voldgade 10, DK-1350 Copenhagen K, Denmark*. E-mail: *ntk@geus.dk*
2) *Department of Earth Sciences, University of Bristol, Bristol BS8 1RJ, UK.*
3) *Department of Earth & Ecosystem Sciences, Lund University, Sölvegatan 12, S-223 62 Lund, Sweden.*

The Fiskenæsset complex in southern West Greenland is part of the North Atlantic craton and is a layered intrusion consisting of gabbro, ultramafic and anorthositic rocks that was deformed during multiple episodes of folding and metamorphism (Myers 1985). We collected late-stage magmatic hornblenditic dykes (Fig. 1) and adjacent anorthosites and studied these samples integratively with several *in situ* techniques to determine the igneous and metamorphic history of the Fiskenæsset complex. Here we report on the first radiometric ages and new mineral chemistry data from anorthosites from the North Atlantic craton in southern West Greenland.

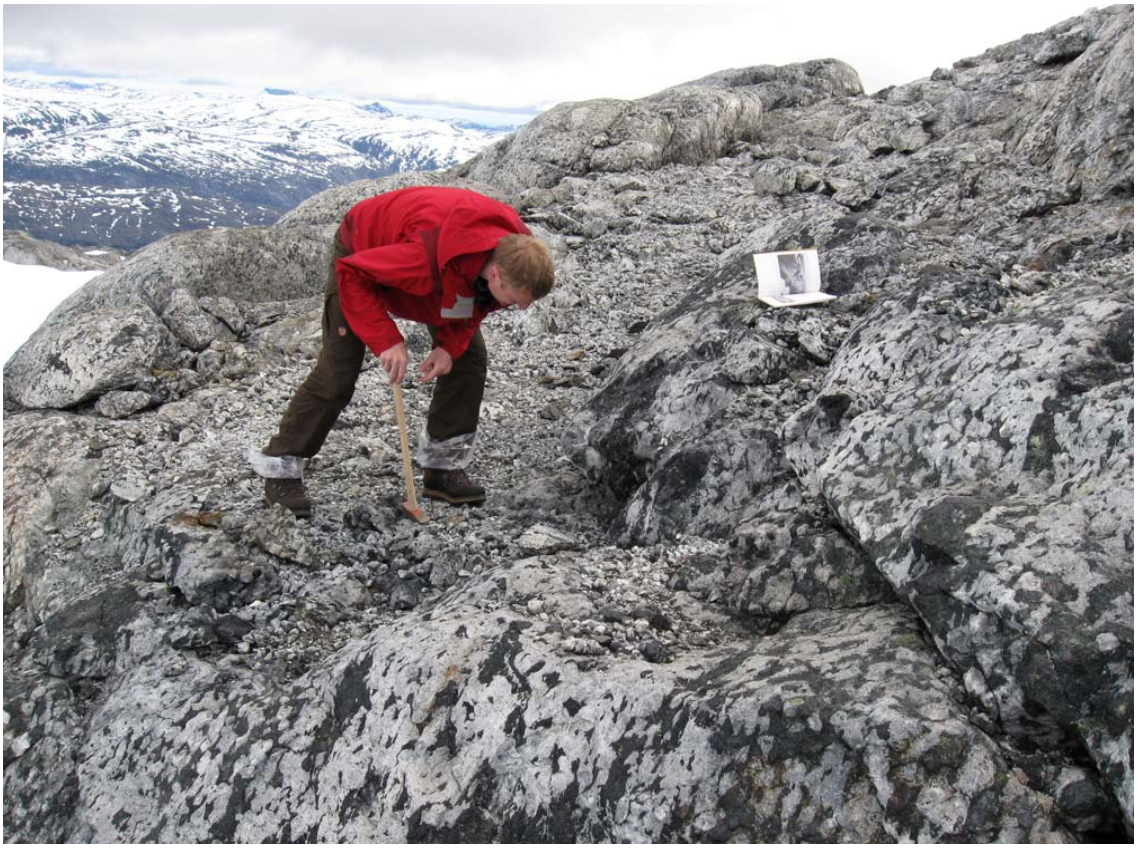

Figure 1. *Magmatic hornblenditic dyke intruding into anorthosite near the peak of Majaqqap Qaava in the Fiskenæsset complex.*

Zircon dating

For U/Pb zircon age determination we selected sample GGU 508216, which consists of hornblenditic dyke material and the surrounding anorthosite rock. The zircons were hand-picked from the heavy mineral fraction of the crushed sample. Age determination was carried out by laser ablation inductively coupled mass spectrometry using an Element2 and NewWave 213 nm UV-laser system at GEUS (Frei & Gerdes 2009).

The zircon spot analyses yielded a wide age span, with $^{207}Pb/^{206}Pb$ ages ranging from 2.70 ± 0.03 to 2.95 ± 0.03 Ga. The oldest zircon grains in our sample are *c.* 2.95 Ga, which probably represents the intrusion age of the anorthosite complex. Consistent with this interpretation are new data by A. Polat and co-workers (pers. comm. 2010): a Sm-Nd isochron intrusion age for the Fiskenæsset complex of *c.* 2.97 Ga and a $^{207}Pb/^{206}Pb$ age of 2.95 Ga. Among the dated hand-picked grains there appear to be two populations, one at 2.92 Ga and another at 2.87 Ga (Fig. 2A). A third possible component at *c.* 2.70 Ga might represent a minor population of metamorphic grains.

In situ observations

To better understand the three zircon forming events (*c.* 2.92, *c.* 2.87 and *c.* 2.7 Ga), we observed the zircon grains *in situ* in polished slabs of the anorthosite samples using the scanning electron microscope at GEUS and the electron microprobe at Copenhagen University. Zircon grains occur in four different textural settings: 1) associated with ilmenite within the hornblenditic dyke, 2) within the hornblenditic dyke, 3) in melt pockets associated with the hornblenditic dyke, and 4) in cracks associated with chlorite (Fig. 2). A further feature in the hornblenditic dyke in the anorthosite is the break down reaction of the ilmenite in the hornblende to form rutile, titanite and chlorite (Fig. 2). We dated zircon grains from these four different settings *in situ* using the same ICP-MS instrument as described above.

Interpretation

Based on the *in situ* observations and measurements, our current understanding of the igneous and metamorphic history of the anorthosite at Majaqqap Qaava is as follows: after intrusion of the anorthosite at *c.* 2.97–2.95 Ga, zircon formed at high-temperature conditions. Some of these zircon grains can be observed next to ilmenite grains; however, no concordant ages were obtained from the *in situ* measurements.

A later thermal event occurred at *c.* 2.92 Ga, which forms the major age component in the zircon population extracted from the crushed sample. Since only one *in situ* zircon measurement yields 2.92 Ga, the true nature of this event is unclear. This age might be related to an igneous event that formed the precursors to the amphibolite units in the area (see e.g. Nutman *et al.* 2004), or the earliest on-set of tonalitic gneiss formation in the region (Næraa & Scherstén, unpubl. data).

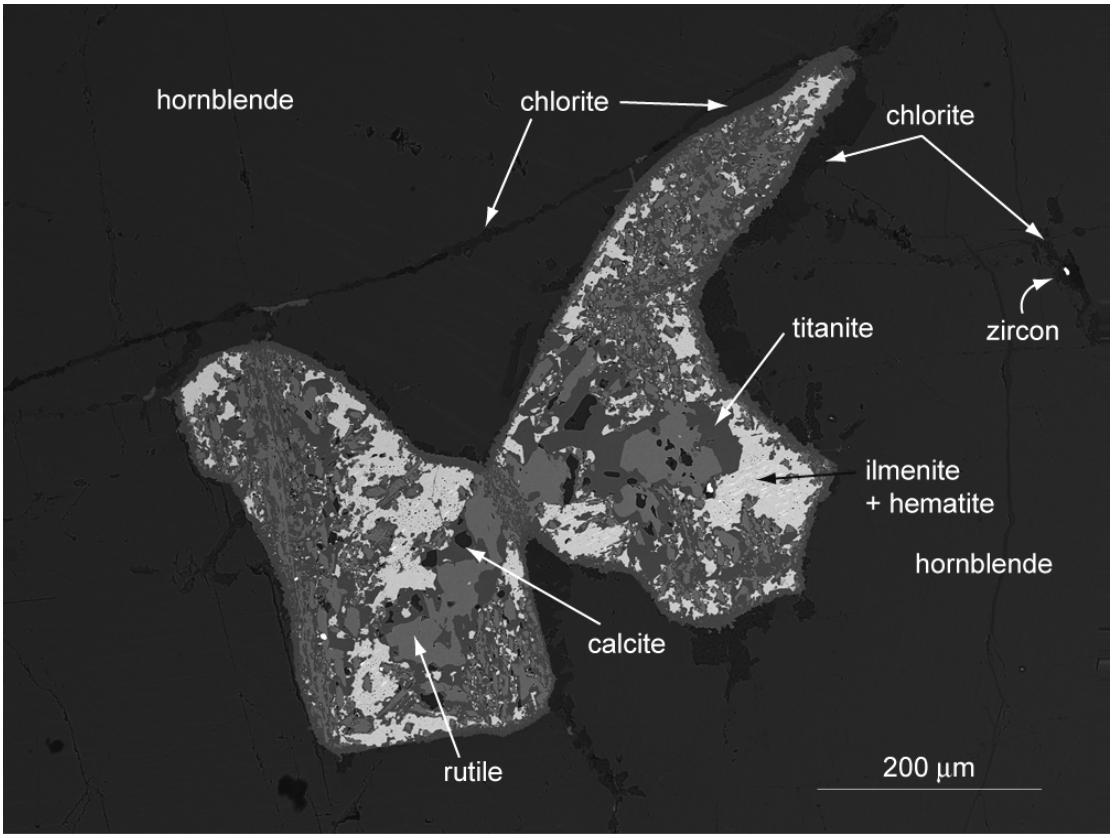

Figure 2. *Back-scatter electron contrast mode scanning electron microscope image showing zircon in chlorite-filled cracks and the break down reaction of ilmenite and hornblende to titanite, rutile and chlorite.*

Zircon grains from the contact region between the hornblenditic dyke and the anorthosite were observed both in relation to melt pockets and as occurring in the amphibole-anorthite assemblages. These different textural settings yield indistinguishable zircon $^{207}Pb/^{206}Pb$ ages of 2.878 ± 0.011 Ga and 2.856 ± 0.016 Ga respectively. There is, however, a large range in ages between the individual analyses. We suggest that this wide age range originates from inheritance or metamorphic overprinting, but the mean age reflects the crystallisation or resetting related to the intrusion of the hornblenditic dykes. The melt pockets in the hornblenditic dykes likely represent their final solidification. If correct, and if this age is representative, it implies that the dykes represent a late magmatic event, much later than previously assumed. This interpretation is at odds with field observations, which are best explained by their intrusion into a partly solidified anorthosite crystal mush rather than a brittle solid. Alternatively, part of the hornblenditic dykes could have remelted during the intrusion of tonalitic gneisses in the area at this time (Nutman *et al.* 2004; Næraa & Schersten 2008). After further cooling hematite lamellae exsolved in the ilmenite and these lamellae are seen as thin needles in the ilmenite grains.

The observed reaction microstructures suggest partial hydration of the assemblage hornblende + ilmenite, which yields the reaction products chlorite + rutile + titanite. This assemblage does not contain quartz. The reaction products are concentrated at the grain boundaries between hornblende and ilmenite, which suggests that the reactions are driven by small amounts of fluid present at the grain boundaries. Since the anorthosites are dry, the extent to which retrograde metamorphic changes can be recorded is a function of the amount of water brought into the system by the hornblenditic dykes. The reactions likely ceased after all the local fluid was consumed. Assuming the reactions took place in an es-

sentially closed system, as water-rich chlorite grew, the composition of the fluid could show considerable variation.

Within the chlorite-filled cracks in the hornblende-rich parts of the sample, newly grown zircons up to 100 µm in length are found. These zircon grains appear to fill the interstitial space between the chlorite-rimmed hornblende grains. The source of zirconium to form these zircons is most probably the ilmenite grains that broke down in the reaction discussed above. The age of the zircon grains in these chlorite-filled cracks is poorly constrained age at 2.70 Ga, but this age is in good accordance with the interpretation that the ilmenite break down reaction occurred shortly after peak metamorphism. Regional metamorphism was previously dated at 2.72 Ga, based on material from the Nuuk region (e.g. Friend *et al.* 1996) and the same age was reported north of Ilivertalik by Næraa & Scherstén (2008).

Modelling of the metamorphic reaction

Modelling of reactions to determine the approximate conditions of formation is complicated by extensive compositional variation of the amphibole and by potential variation in the fluid composition. Nevertheless, using *PerPlex* (Connolly 2005) it is possible to locate mineral composition isopleths that approximate microprobe data for the amphibole and chlorite.

The *PerPlex* modelling results are shown in figure 3. These results fit well with peak metamorphic conditions suggested in Keulen *et al.* (2009). The reaction seems to have occurred just after peak metamorphic conditions at about 600°C and after peak metamorphism in the area.

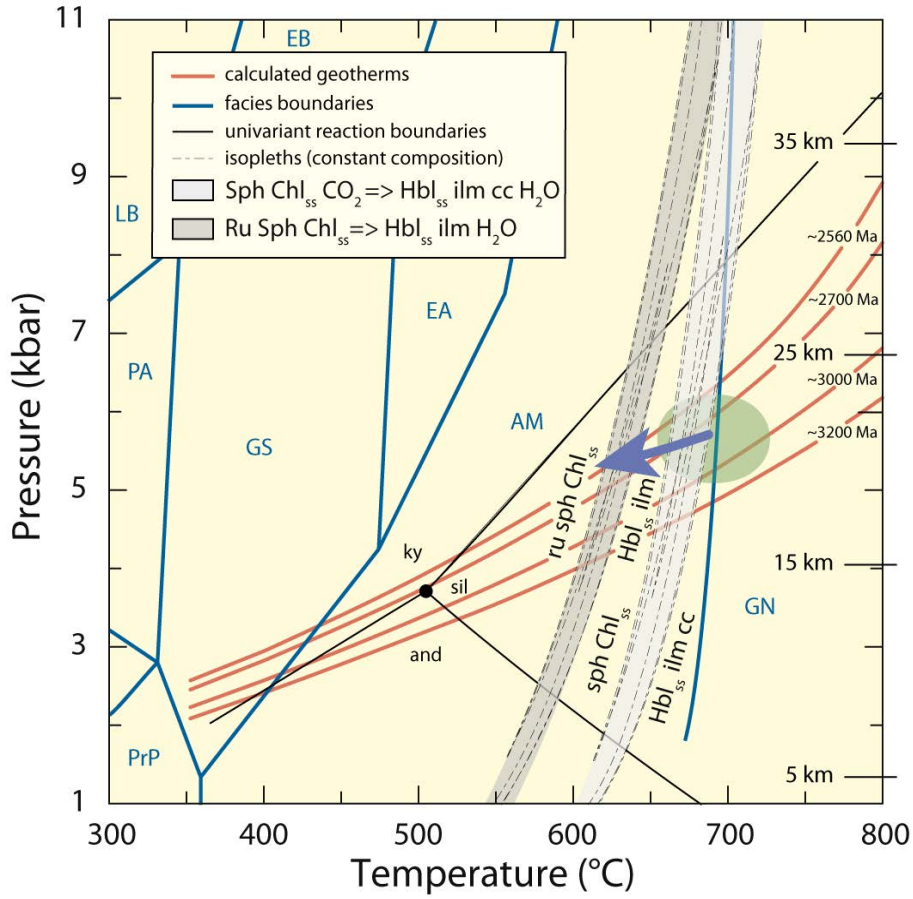

Figure 3. *Pressure-temperature (P–T) diagram that shows ranges of P–T estimates for modelled compositions of chlorite (X_{Mg}=0.81-0.84) and hornblende (X_{Mg}= 0.70-79; Al (apfu) =1.490-1.626); geotherms based on measured contents and estimated contents as a function of time of radiogenic elements in basaltic and felsic Greenland rocks. The calculations are based on a crustal thickness of 40 km and use a two-layer model with 10 km of mafic rocks at the base of the crust overlain by 30 km of felsic rocks. Depths in kilometres are based on an average crustal density of 2.75 g/cm^3. Parameters: mantle heat flow: 20 mW/m^2; mafic and felsic rock heat production respectively are: 0.262 and 3.478 µW/m^3 at 3.2 Ga (possible maximum age for this part of the terrane), 0.244 and 3.254 µW/m^3 at 3.0 Ga, 0.220 and 2.945 µW/m^3 at 2.7 Ga, 0.210 and 2.811 µW/m^3 at 2.56 Ga (age of the Qôrqut Granite). The pale-green area are the peak P-T conditions suggested by Keulen et al. (2009). The blue arrow is part of a possible cooling path. Abbreviations:* ***AM*** *= amphibolite facies;* ***EA*** *= epidote-amphibolite facies;* ***EB*** *= epidote-blueschist facies;* ***LB*** *= Lawsonite-blueschist facies;* ***GN*** *= granulite facies;* ***GS*** *= greenschist facies;* ***PA*** *= Pumpellyite-actinolite facies;* ***PrAc*** *= Prehnite-actinolite facies;* ***AND*** *= andalusite;* ***Cc*** *= calcite;* ***Chl$_{ss}$*** *= chlorite solid solution;* ***Hbl$_{ss}$*** *= hornblende solid solution;* ***Ilm*** *= ilmenite;* ***KY*** *= kyanite;* ***Ru*** *= rutile;* ***SIL*** *= sillimanite;* ***Sph*** *= sphene (titanite).*

As a result of this pilot study on zircon grains and their surrounding minerals in samples from Majaqqap Qaava within the Fiskenæsset complex, southern West Greenland, we are able to show that the anorthosite records a metamorphic history that is more complex than previously recognised. Careful *in situ* observations prove helpful in unravelling the history of these rocks.

References

Connolly, J.A.D. 2005: Computation of phase equilibria by linear programming: A tool for geodynamic modeling and its application to subduction zone decarbonation. Earth and Planetary Science Letters **236**, 524–541.

Frei, D. & Gerdes, A. 2009: Precise and accurate *in situ* U–Pb dating of zircon with high sample throughput by automated LA-SF-ICP-MS. Chemical Geology **261**, 261–270.

Friend, C.R.L., Nutman, A.P., Baadsgaard, H, Kinny, P.D. & McGregor, V.R. 1996: Timing of late Archaean terrane assembly, crustal thickening and granite emplacement in the Nuuk region, southern West Greenland. Earth and Planetary Science Letters **142**, 353–365.

Keulen, N., Scherstén, A., Schumacher, J.C., Næraa, T. & Windley, B.F. 2009: Geological observations in the southern West Greenland basement from Ameralik to Frederikshåb Isblink in 2008. Geological Survey of Denmark and Greenland Bulletin **17**, 49–52.

Myers, J.S. 1985: Stratigraphy and structure of the Fiskenæsset complex, southern West Greenland. Bulletin Grønlands Geologiske Undersøgelse **150**, 72 pp.

Næraa, T. & Scherstén, A. 2008: New zircon ages from the Tasiusarsuaq terrane, southern West Greenland. Geological Survey of Denmark and Greenland Bulletin **15**, 73–76.

Nutman, A.P., Friend, C.R.L., Barker, S.L.L. & McGregor, V.R. 2004: Inventory and assessment of Palaeoarchaean gneiss terrains and detrital zircons in southern West Greenland. Precambrian Research 135, 281–314.

Structural Geology of the Grædefjord area, southern West Greenland

Alexander Kisters (1), Anders Bergen (2), Thomas F. Kokfelt (3), Jochen Kolb (3)

(1) Department of Earth Sciences, University of Stellenbosch, South Africa
(2) Department of Geography and Geology, University of Copenhagen, Denmark
(3) Geological Survey of Denmark and Greenland, GEUS

Structural, metamorphic and, in particular, geochronological data suggest SW Greenland to be made up of a number of distinct tectonostratigraphic terranes or crustal blocks (e.g. Nutman *et al.* 1989; Crowley 2002; Windley & Garde 2009). The area around the Grædefjord has, in recent years, been likened to a suture zone that accommodated the accretion of the northern Sermilik block (the Tasiusarsuaq terrane) against the southern Bjørnesund block (Windley & Garde 2009). This work reports structural and geochronological results collected during the 2009 field season in the Grædefjord region.

The areas surrounding the Grædefjord are dominated by TTG phases (> 90-95 vol.%). Supracrustal rocks include mainly massive to banded amphibolites with very subordinate ultramafic rocks, felsic volcanics and/or volcanoclastics and metasediments. Primary volcanic textures are rare and have been overprinted by pervasive tectonic fabrics. However, felsic (Qtz-Fsp-Ms) schists contain textural evidence that may point to their origin as crystal tuffs and/or volcanoclastic rocks. The voluminous TTG suite shows a regionally developed intrusive sequence. Earliest intrusives are grey, banded TTG gneisses, henceforth referred to as 'grey gneisses'. Intrusive relationships and compositional and textural variations point to the polyphase intrusive history of the early grey gneisses. This was followed by mainly sheet-like leucogranite gneisses and pegmatoids and late-stage pegmatites. The ca. 2.8 Ga Illivertalik Granite along the NE parts of the Grædefjord is a texturally and compositionally very heterogeneous pluton in the NE of the Grædefjord. Based on intrusive relationships, its relative age is between that of the early grey gneisses and later leucogranites.

Rocks in the Grædefjord show evidence of at least three main phases of high-grade, ductile deformation (D1-D3) commonly accompanied by the emplacement of melts, either as in-situ melts or as intrusive stringers, pockets, or regionally mappable granite sheets. A retrograde ductile-brittle deformation (D4) is characterised by the formation of up to 200 m wide, E-W trending mylonite-cataclasite zones and brittle, mainly northerly-trending faults (D5).

The earliest phase of deformation (D1) consists of early recumbent folds and a layer-parallel transposition. This phase is only observed in supracrustals and the early grey gneisses. On a regional scale, D1 is indicated by a type 3 fold interference pattern outlined by supracrustal belts that suggests an early recumbent fold phase refolded by a subsequent upright fold phase (F2). In the Grædefjord, relics of the probably early horizontal fabric domains are locally preserved in low-strain domains.

The D2 deformation comprises a second fold phase characterised by upright, N-S trending, mainly steeply plunging folds (F2). Mesoscopic F2 folds are well preserved in low-

strain domains immediately S of the Grædefjord. Volumetrically subordinate but abundant leucogranites intrude axial planar to F2 folds. On a more regional scale, the northerly-trending folds form a type 3 fold interference with early F1 folds outlined by amphibolite belts.

The D3 deformation is the main fabric-forming event that dominates the structural grain of the central Grædefjord region. D3 is characterised by E-W trending, upright, steeply plunging folds that refold F2 folds. In D3 high-strain zones, all earlier fold generations (F1-F3) are completely transposed into a subvertical, E-W trending gneissosity. Fabric development indicates that D3 strains are characterised by bulk N-S subhorizontal shortening. Layer-normal shortening is associated with a steep stretch and foliation-parallel extension, indicated by shear bands and the near ubiquitous steep SE- to E-plunging mineral stretching lineation. In places, prolate fabrics are dominant. Deformation is accompanied by the emplacement of the main phase of commonly sheet-like leucogranites and pegmatites that intrude axial planar to F3 folds or parallel to the E-W trending gneissosity (S3). Despite the high-strain fabrics, mylonitic textures are rare, signifying the high T-conditions of deformation and the presence of melts in the rocks, both facilitating recovery processes. D3 high-strain fabrics (gneiss belts, striped gneisses and interlayered amphibolites) dominate the area around the Grædefjord. Away from the central high-strain belts, D3 strains are interpreted to have resulted in the refolding of earlier fabrics (D2 and D3) by kilometer-scale, steeply-plunging, parallel to the regional stretch, tubular (sheath?) folds (D3 late). These folds are interpreted to have formed in response to the vertical extrusion of material on the margins of the D3 high-strain Grædefjord structure.

The D4 deformation is characterised by the formation of E-W trending, subvertical to steep N dipping ductile-brittle high-strain zones, characterised by pervasive crystal-plastic textures in mylonite zones next to and overprinted by brittle-ductile cataclasites. The high-strain zones show a close spatial association with late-stage pegmatites and leucogranites. Kinematic indicators point to predominantly dextral strike-slip kinematics, although top-to-the-S reverse movement and top-to-the-N normal movement were also recorded. In places, D4 shear zones are associated with SE verging folds.

The last deformation (D5) is characterised by the formation of brittle faults. D5 faulting is particularly widespread in coastal outcrops in the W. Here, the faults are invariably steep, N-S trending or defining a conjugate pattern around N trends, corresponding to an episode of E-W extension. Faulting occurred under low-grade metamorphic conditions, indicated by the formation of breccias, non-cohesive cataclasites, quartz veining and associated chloritisation and sericitisation of surrounding wall-rocks.

Geochronological work was aimed at constraining the absolute timing of plutonic episodes and deformational events and field observations correlate very well with the geochronological results. At least two phases of early grey gneisses can be identified in the field, the oldest of which yielded an age of 2912 ± 3 Ma, whereas a younger phase yielded an age of 2811.3 ± 4.3 Ma, both of which are interpreted as the crystallisation ages of the TTG gneisses. The relationship between the older grey gneiss and amphibolites could not be established with certainty since the contacts between the two are invariably tectonised and transposed. The younger grey gneiss phase is, however, intrusive into the older gneisses and amphibolites, so that the supracrustals must be assumed to be at least 2800 Ma in age. Younger, syn-D3 leucogranites have been dated from both sides of the Grædefjord. They show a very close cluster around ages of ca. 2710 Ma (2711.3 ± 4.8 Ma, 2701 ± 7 Ma and 2708 ±2 Ma), constraining the timing of the D3 deformation in the Grædefjord area. A sample of late-stage pegmatites yielded an age of 2625 ± 9 Ma.

Theoretical considerations and modeling of hot and, as a consequence, rheologically weakened crustal structures during collisional tectonics (e.g. Touissant *et al.* 2004) predict bulk flow of the weak crustal levels rather than crustal stacking and deformation localised along discrete thrusts or detachments. This agrees well with the bulk shortening and vertical extrusion of high-grade quartzofeldspathic gneisses in the Grædefjord that are, moreover, intruded by volumetrically abundant granitic melts during deformation at ca. 2710 Ma. Lateral displacement of units or nappe emplacement are, at least at this structural level, not recorded. The timing of deformation in the Grædefjord corresponds to the well-documented phase of late-Archaean accretionary tectonics along the northern margin of the Sermilik block (Tasiusarsuaq terrane). The timing and structural style along the D3 structure may correspond to an intraplate deformation zone, in which rheologically weakened crust records far-field stresses related to e.g. collisional processes at plate-boundaries at ca. 2700 Ma to the north, rather than a terrane boundary sensu stricto.

References

Crowley, J.L. 2002: Testing the model of late-Archean terrane accretion in southern West Greenland: a comparison of the timing of geological events across the Quarlit Nunaat fault, Buksefjorden region. Precambrian Research **116**, 57-79.

Nutman, A.P., Friend, C.R.L., Baadsgaard, H. & McGregor, V.R. 1989: Evolution and assembly of Archean gneiss terranes in the Godthabsfjord region, southern West Greenland: structural, metamorphic and isotopic evidence. Tectonics **8**, 573-589.

Touissant, G., Burov, E, & Jolivet, L. 2004. Continental plate collision: Stable vs unstable slab dynamics. Geology **32**, 33-36.

Windley, B.F. & Garde, A.A. 2009. Arc-generated blocks with crustal sections in the North Atlantic craton of West Greenland: new mechanism of crustal growth in the Archaean with modern analogues. Earth Science Reviews **93**, 1-30.

Thematic age distribution maps of the Archaean basement of southern West Greenland

Thomas F. Kokfelt, Nynke Keulen, Tjerk C. Heijboer, Tomas Næraa, Anders Scherstén

The Archaean basement of southern West and South West Greenland is dominated by orthogneiss, or so-called TTG (Tonalite, Trondhjemite, Granodiorite) gneisses, that constitute about 90% of the present day surface area. Dispersed within the gneisses are older 'greenstone belts' that are the presumed remnants of volcanic arcs (e.g., Steenfelt et al., 2005; Windley & Garde, 2009). The greenstone belts mainly comprise amphibolites, mafic granulites and anorthosites, with subordinate metasediments (or mica schists) and ultramafic rocks, and are intruded by later TTG melts. The basement was subsequently deformed and metamorphosed under amphibolite to granulite facies conditions. Evidence of late-stage magmatic activity in the area is indicated by undeformed pegmatites that intrude all lithologies.

The Archaean basement in Southern West and South West Greenland has been divided into various terranes or blocks that each represents architectural components with presumed distinct geological histories. Each terrane or block represents mid to deep-crustal sections of crust that was generated in an arc-related setting. The proposed terranes are largely defined based on geochronological data (Friend et al., 1996; Crowley, 2002; Friend & Nutman, 2005).

The block model of Windley & Garde (2009), suggests that the Archaean basement consists of six blocks, from north to south: the Maniitsoq, Fiskefjord, Sermilik, Bjørnesund, Kvanefjord and Ivittuut blocks (Windley & Garde 2009). Some of these blocks are composed of several terranes (Friend et al. 1996). Each block is tilted variably southwards, leading to a pattern of progressively higher metamorphic grade to the north within each block. The upper crustal zone consists of prograde amphibolite metamorphic facies rocks, whilst the lower crustal zone consists of retrograde amphibolite and granulite facies metamorphic rocks (Windley & Garde 2009).

In this paper we present a preliminary interpretation of a large new regional age dataset from the Sermilik and Bjørnesund blocks between 62º30'N and 64º00'N. The radiometric U-Pb ages were obtained on zircons from 87 rock samples, comprising orthogneisses (TTG's), granites, pegmatites, quartz-diorites and anorthosites. In addition 12 stream sediment samples from the same area were included.

The age dates were obtained at GEUS on a LA-ICPMS (laser ablation inductively coupled plasma mass spectrometer) facility that comprise a New Wave 213 nm UV laser and an Element2 ICP-MS (Finnigan) (Frei & Gerdes, 2009). Zircon separation was done on a Wilfley table, and the zircons were embedded in an epoxy mount that was abraded and polished to expose the centre of each grain. The zircons were examined and imaged on the SEM (scanning electron microscope) by the use of back-scattered electrons, in order to document the internal structure of the zircons (zoning patterns, inclusions, etc.).

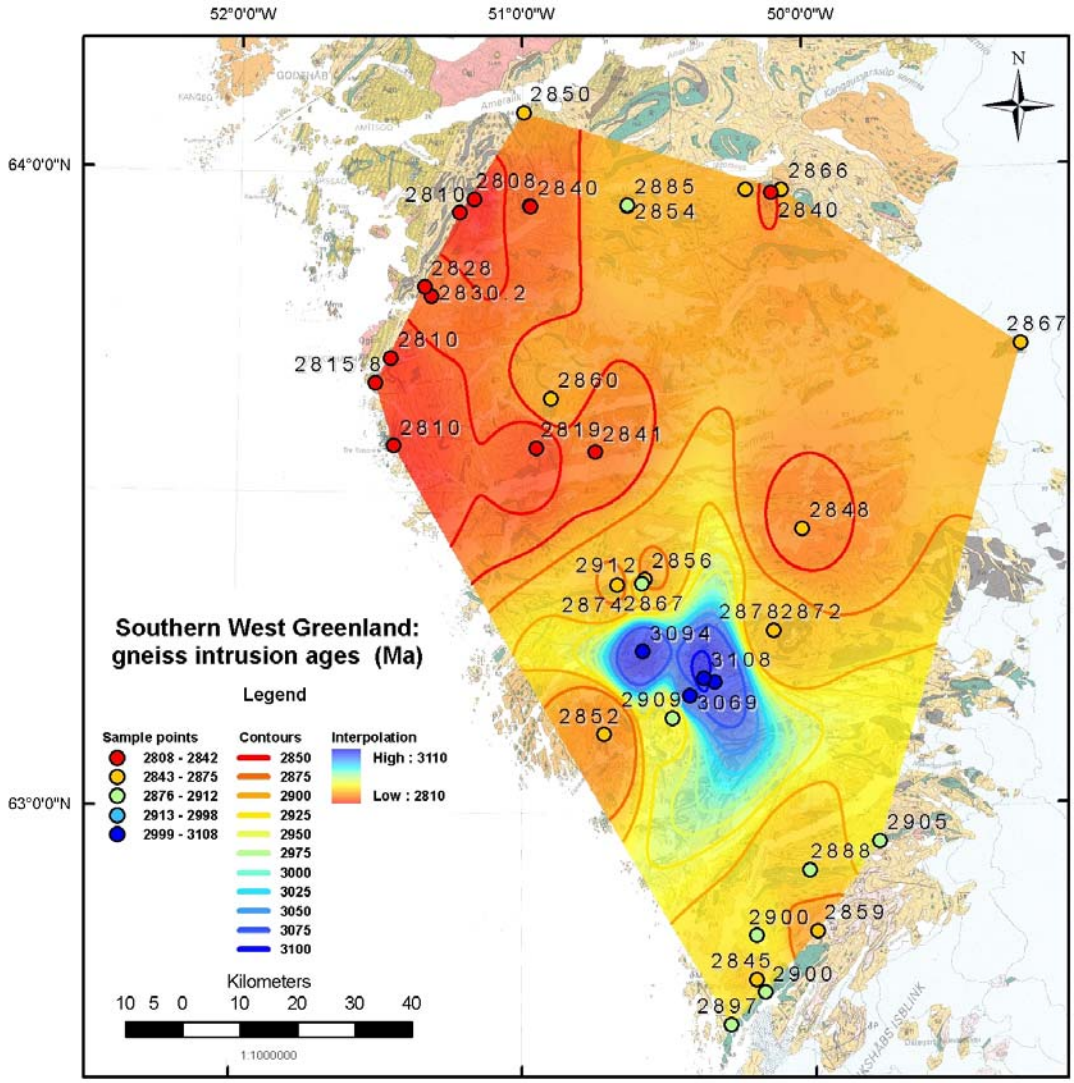

Figure 1. *Gneiss formation ages in the Sermilik and Bjørnesund blocks. Gneiss formation ages are systematically younger in the north. Very old gneisses are found in a restricted area around Fiskenæsset Fjord. A TIN (triangulated irregular network) interpolation of these points was constructed with IDRISI and ArcGIS to identify general age trends. Angular contour segments are relics of the interpolation procedure.*

A large number of zircon grains (i.e., 50-150, usually about 100) were analysed per sample in order to obtain a sufficient statistical basis for identifying individual age peaks in samples exhibiting multiple age components. Interpretation of zircon ages was in part based on visual inspection of zircon types from BSE images, e.g., distinguishing primary magmatic from metamorphic, zircons, and in part from geochemistry, e.g., from any systematic variations of $^{207}Pb/^{206}Pb$ age with Th/U and U concentration of the zircons. Following data reduction, the Excel add-on program 'Isoplot' by Ludwig (2003) was used to plot the data. For the interpretation of complex age patterns and for the unravelling of distinct age populations we used the 'unmix' function of 'Isoplot' program, which provides a least squares residual approach to fit the data into any given number of age peaks.

The main findings from our compiled age data set are as follows:

- Gneisses north of the Grædefjord deformation zone are generally younger than 2.87 Ga, whereas those south of this deformation zone are generally older than 2.87 Ga.
- The Tasiusarsuaq terrane appears to end just south of the Grædefjord.
- Very old gneisses (3.1 Ga) occur in the Fiskenæsset Fjord area.
- 3.1-3.2 Ga ages are found regionally as inherited zircon grains.
- An age of 2.82-2.80 Ga for granulite facies metamorphism is found in the area around the Ilivertalik granite.
- In the Bjørnesund-Ravn Storø area, the main deformation event occurs at ca. 2.85-2.83 Ga.
- In the area west and north of the Ilivertalik granite the main deformation occurs ca. 2.78-2.75 Ga, this deformation event is not observed in the area NW of Buksefjorden, nor SE of the Ilivertalik granite.
- A regional deformation event occurred at 2.74-2.70 Ga in the entire area, corresponding to the main deformation event in the northern area, but the late deformation in the southern area.

References:

Frei, D. & Gerdes, A. (2009). Precise and accurate *in situ* U-Pb dating of zircon with high sample throughput by automated LA-SF-ICP-MS. Chemical Geology 261, 261-270.

Friend, C.R.L. & Nutman, A.P. (2005). New pieces to the Archaean terrane jigsaw puzzle in the Nuuk region, southern West Greenland: steps in transforming a simple insight into a complex regional tectonothermal model. Journal of the Geological Society (London) 162, 147-162.

Friend, C.R.L., Nutman, A.P., Baadsgaard, H., Kinny, P.D. & McGregor, V.R. (1996). Timing of late Archaean terrane assembly, crustal thickening and granite emplacement in the Nuuk region, southern West Greenland. Earth and Planetary Science Letters 142, 353-365.

Ludwig, K.R. 2003: Mathematical-statistical treatment of data and errors for Th-230/U geochronology. Uranium-Series Geochemistry, Reviews in Mineralogy and Geochemistry 52, 631–656.

Steenfelt, A., Garde, A.A. & Moyen, J.-F. (2005). Mantle wedge involvement in the petrogenesis of Archaean grey gneisses in West Greenland. Lithos 79, 207-228.

Windley, B.F. & Garde, A.A. (2009). Arc-generated blocks with crustal sections in the North Atlantic craton of West Greenland: new mechanism of crustal growth in the Archaean with modern analogues. Earth Science Reviews 93, 1-30.

On the occurrence of baddeleyite in zircon in silica-saturated metamorphic rocks

Alexander Lewerentz[1], Nynke Keulen[2], Thomas F. Kokfelt[2], Anders Scherstén[1]

1) *Dept. of Earth & Ecosystem Sciences, Lund University, Sölvegatan 12, 223 62 Lund, Sweden, alexander.lewerentz@gmail.com*
2) Geological Survey of Denmark & Greenland, Øster Voldgade 10, 1350 Copenhagen K, DK

Baddeleyite (ZrO_2) is an important mineral for U-Pb geochronology in silica undersaturated rocks. Under silica saturated conditions, baddeleyite reacts to form zircon along the reaction:

$$ZrO_2 + SiO_2 \rightarrow ZrSiO_4 \qquad [Eq.\ 1]$$

Yet, we document baddeleyite domains within zircon in several quartz-saturated rock types from southern West Greenland. In order to explain the observations of baddeleyite in zircon derived from granite, felsic pegmatite and possibly meta-sedimentary rocks; the primary aim of this project is to make detailed petrographical and textural descriptions of the phenomenon. In this manner, we hope to better understand the origin of baddeleyite. Is the baddeleyite of primary magmatic origin, or an effect of secondary alteration, i.e. can the baddeleyite to zircon reaction be reversed (Eq. 1)? Is there any link to regional geology or to the presence of detrital baddeleyite grains? To the extent possible, we are also linking these observations to existing U-Pb data on the zircon fractions.

A range of methods was applied to study the samples. Polarisation microscopy was used to establish the in situ textural setting of zircon grains. Back-Scattered Electron mode Scanning Electron Microscopy (SEM-BSE) was used to describe structural and textural relationships within the zircons and with respect to neighbouring grains. Energy Dispersive X-ray Spectroscopy (EDS) was used to measure any compositional differences within the grains. SEM-EDS analyses were made *in situ,* on grains in thin sections and on mounted grains in epoxy mounts.

Baddeleyite-bearing zircon grains occur in quartz, plagioclase, biotite and in contact with apatite. These zircon grains occur most abundantly in quartz, and in some cases the baddeleyite domain is in contact with quartz. There are two different textural occurrences of these baddeleyite domains; as bands concordant with the primary zircon zonation, and as patchy irregular blob-like domains (Fig. 1).

The baddeleyite domains are impure. They are not silica-free, though this could be a disturbance effect from underlying zircon. Minor amounts of trace elements, such as uranium and hafnium, are also detected within the baddeleyite. The most striking observation however, is the detection of aluminium, calcium and iron in the baddeleyite. Towards each baddeleyite domain, zircon often becomes darker in BSE. EDS-analyses demonstrate that the darker zircon is impure; containing minor amounts of non-stoichiometric elements, such as calcium, iron, sodium and titanium. The part of the zircon grain outside the baddeleyite domain is often abundantly fractured. The fractures usually stop at or near the outer

boundary of the baddeleyite domain. This pattern correlates especially well for the patchy irregular baddeleyite occurrences.

Here we propose a preliminary explanation for each of the two end-member types of occurrences. For the occurrences of baddeleyite that are concordant with the primary zonation, we suggest that variation in silica activity in the magma is the cause for the presence of baddeleyite. This would make the magma crystallise zircon when the silica activity is high and baddeleyite when the magma is temporarily or locally silica undersaturated. A possible process could be replenishment and mixing of a fractionated (silica-rich) magma with a primitive (silica-poor) magma batch in the magma chamber. In contrast, we suggest that the occurrences of patchy irregular domains are due to later hydrothermal alteration of the zircon grains. This model is supported by the fracture patterns associated with this type of occurrence of baddeleyite, and also by their anheadral habitus.

To further investigate this phenomenon and reach a more solid theory, some future work is needed. For example, precise and accurate U-Pb geochronology of zircon and baddeleyite domains will provide important clues to the origin and timing of baddeleyite generating events. Linking baddeleyite formation with metamorphism will probably provide important clues about metamorphic fluid chemistry and reactions during various metamorphic stages. U-Pb age data should ideally be linked with O-Hf data, which might provide further evidence on the origin and on metamorphic fluids.

Figure 1. *BSE-image of a zircon, where the grey areas are zircon, black spots slightly impure quartz inclusions and white areas baddeleyite (with the exception of two spots that mainly consist of U, Th and Pb). This grain shows both types of occurrences, as well as fractures associated with the area near patchy irregular baddeleyite domains (in the right part of the grain). It is notable that some of the patchy irregular baddeleyite domains are in direct contact with quartz inclusions.*

U-Pb ages of mafic intrusions in the North Atlantic Craton, and implications for a palaeoreconstruction

Mimmi K.M. Nilsson[a,1], Ulf Söderlund[a], Richard E. Ernst[b,2,3], Michael A. Hamilton[c], Anders Scherstén[a], Paul E.B. Armitage[d]

[a] Department of Geology, GeoBiosphere Science Centre, Lund University, Sölvegatan 12, SE-223 62 Lund, Sweden, [b] Geological Survey of Canada, 601 Booth Street, Ottawa, Ontario, Canada K1A 0E8, [c] Department of Geology, University of Toronto, Toronto, Canada ON M5S 3B1, [d] Nunaminerals A/S, P.O. Box 790, Nuuk DK-3900, Greenland

Present address: [1]Department of Geology, GeoBiosphere Science Centre, Lund University, Sölvegatan 12, SE-223 62 Lund, Sweden. E-mail: mimmi.nilsson@geol.lu.se, Tel: 46-46-2229553. Fax: 46-46-2224419, [2]Ernst Geosciences, 43 Margrave Avenue, Ottawa, Canada K1T 3Y2, [3]Dept. of Earth Sciences, Carleton University, Ottawa, Canada K1S 5B6.

The collective masses of Archaean coastal bedrock exposures in Labrador (Nain Province), western and eastern South Greenland, and the Lewisian complex of Scotland together comprise the North Atlantic craton (NAC) (e.g. Bridgwater et al., 1973). The exposed Archaean bedrock of southern Greenland has been intruded by numerous generations of mafic dyke swarms, as evident from differing trends and cross-cutting relationships. However, only a subordinate number of these dykes have been dated by modern radiometric techniques such as the U-Pb method on zircon or baddeleyite. In this study we present four U-Pb ID-TIMS baddeleyite ages of mafic dykes from the North Atlantic Craton, and one U-Pb zircon LA-ICPMS age for a mafic-ultramafic intrusion in SW Greenland (summarised in Table 1).

The northern margin of North Atlantic Craton in Greenland is intruded by a NNE-E trending dyke swarm collectively termed the Kangâmiut dykes, which are variably reworked by c. 1.9-1.8 Ga Nagssugtoqidian deformation. Kangâmiut dykes have yielded U-Pb zircon ages of 2036 ± 5 Ma, 2046 ± 8 Ma (Nutman et al., 1999) and 2048 +4/-2 Ma (Connelly et al., 2000). In addition, one dyke from southern East Greenland, likely to correspond to the Kangâmiut dykes, was dated at 2015 ± 15 Ma (Nutman et al., 2008; revised from a 2048 ±17 Ma age quoted in Nutman et al., 1999).

Further to the south in SW Greenland, mafic dyke swarms termed 'BN' (boninitic-noritic) and 'MD' (meta-dolerite) dykes are recognised (Hall & Hughes, 1987). Three subswarms of the MD dykes have been distinguished, termed MD1, MD2 and MD3. The ages of the MD dykes are poorly known; Kalsbeek & Taylor (1985) reported Rb-Sr ages of 2180 ± 100 Ma (MD2), and 2110 ± 135 Ma and 2080 ± 110 Ma (both MD3).

Table 1. Description of U-Pb dated samples

Sample name	Interpreted unit	Latitude	Longitude	Direction	Age, error (2σ)
Sample A	Amikoq layered intrusion	64°55'40.65"N	51°25'37.89"W		2990 ± 13
499217	Kilaarsarfik dyke	64° 6'42.34"N	49°51'7.66"W	Not recorded	2499.3 ± 1.6
515805	MD3 dyke, Ravn Storø	62°40'29.79"N	50°15'24.54"W	WNW	2050.2 ± 2.0
515830	MD3 dyke, inner Bjørnesund	63° 2'47.35"N	49°44'1.56"W	WNW	2040.7 ± 3.1
468749	MD3 dyke, Sermilik Fiord	63°25'52.58"N	51° 1'31.75"W	E-W to WNW	2029.0 ± 3.0
HMB96-127	Iglusuataliksuak dyke	57° 2' 10.67"N	62° 2' 6.80"W	SE	2044.7 ± 1.7

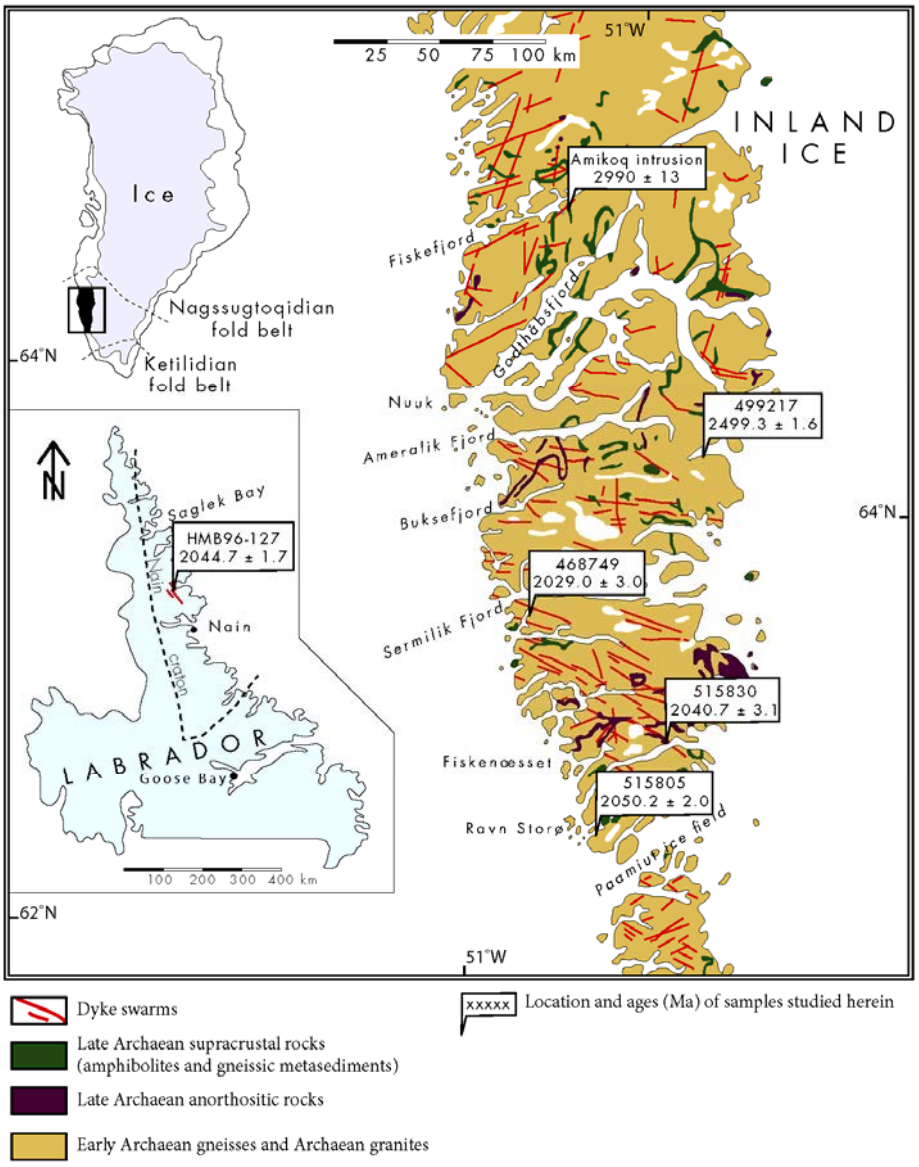

Figure 1. *Simplified geological map of SW Greenland showing the occurrences and principle trends of mafic dykes, sample locations and ages presented herein. Modified after Nilsson et al. (in press), Escher and Pulvertaft (1995) and Hall and Hughes (1987). The inset map of Labrador shows the sample location of the herein revised age of the Iglusuataliksuak dyke is modified after Buchan and Ernst (2004).*

Herein we present U-Pb baddeleyite ages of three WNW-trending mafic dykes from SW Greenland, interpreted as members of MD3 dykes: 2050 ± 2 Ma (GGU nr. 515805), 2041 ± 3 Ma (515830) and 2029 ± 3 Ma (468749) (all errors 2σ). In addition we also present a revised age of a Iglusuataliksuak dyke from Nain Province, Labrador at 2045 ± 2 Ma (Fig. 1). These new ages together with present U-Pb data of Kangâmiut dykes suggest that the Kangâmiut-MD3- Iglusuataliksuak swarms are components of a single generation of dykes, intruded over a protracted period of c. 30 Ma. We further speculate that these dykes could define a radiating dyke swarm (corrected for opening of the Labrador Sea) that manifests the arrival of a mantle plume centered on the western margin of the North Atlantic Craton.

One mafic dyke occurring among the c. 2040 Ma generation of Kangâmiut dykes have yielded an $^{40}Ar/^{39}Ar$ age of c. 2.5 Ga (Willigers et al., 1999), indicating the presence of an

older generation of dykes in the Kangâmiut area. The U-Pb (ID-TIMS, baddeleyite) age of a dyke located SE of Ameralik Fjord (c. 250 km south of the Kangâmiut area proper) yields an age of 2499 ± 2 Ma, hence corroborating the Ar/Ar result. We propose the name Kilaarsarfik dykes for c. 2500 Ma dykes in SW Greenland in order to distinguish them from the intermixed 2050-2030 Ma Kangâmiut – MD3 dykes.

Comparison of magmatic 'barcodes' from the Nain and Greenland portions of the North Atlantic Craton with the north-eastern Superior Craton reveals multiple matches at ~2500, ~2214, 2050-2030 and ~1950 Ma. These matches allow for a tentative reconstruction of the North Atlantic Craton proximal to the northeastern margin of the Superior Craton in the late Archaean-Palaeoproterozoic (Fig. 2). Zircon dating by LA-ICPMS has also defined an emplacement age of 2990 ± 13 Ma (mean $^{207}Pb/^{206}Pb$ age) for the extensive, ultramafic-mafic Amikoq intrusion in the central Fiskefjord area.

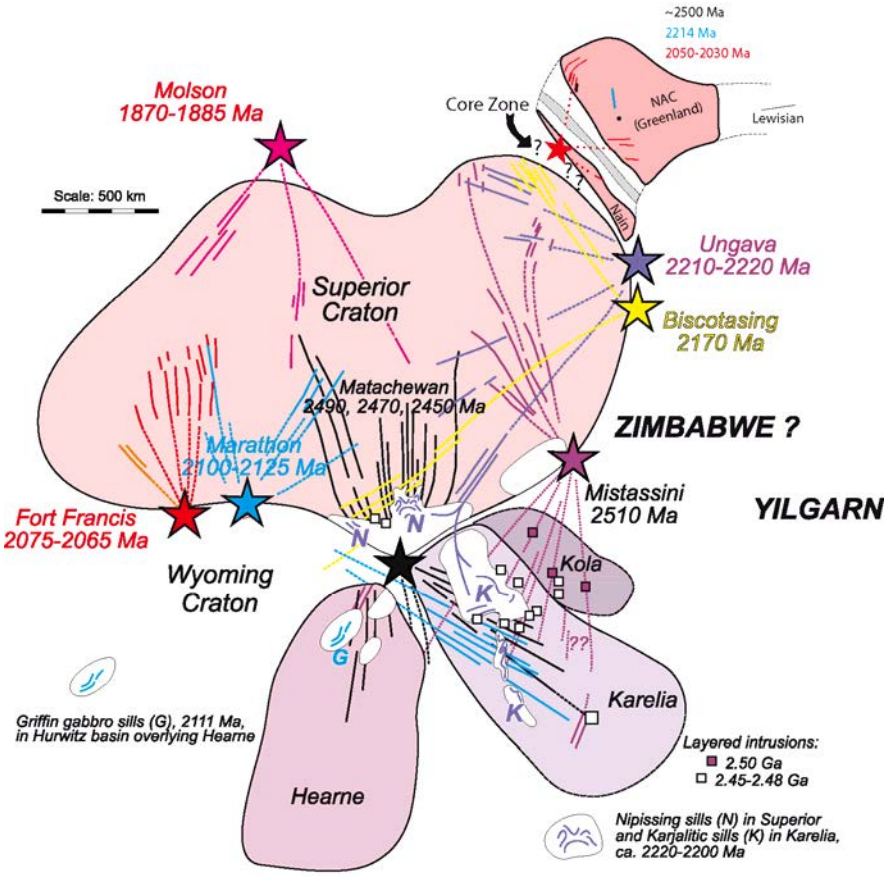

Figure 2. *Possible Paleoproterozoic reconstruction of Greenland and Nain craton in a nearest neighbour situation to Superior craton, with earlier reconstructions of Kola-Karelia, Hearne and Wyoming cratons using the LIP record (modified after Bleeker and Ernst, 2006). Note that Zimbabwe and Yilgarn are tentatively positioned (cf. Söderlund et al., in press). Further reconstructions would be possible by additional high-precision age determinations of the c. 2200 Ma dykes of SW Greenland. The possible match between these dykes and the 2210-2220 Ma Ungava dyke swarm could provide a major constraint and a definite reconstruction.*

References

Bleeker, W., Ernst, R., 2006. Short-lived mantle generated magmatic events and their dyke swarms: The key unlocking Earth's paleogeographic record back to 2.6 Ga. Dyke Swarms - Time Markers of Crustal Evolution, 3-26.

Bridgwater, D., Escher, A., Watterson, J., 1973a. Tectonic displacements and thermal activity in two contrasting Proterozoic mobile belts from Greenland. Philos. Trans. Royal Soc. London, A273, 513–533.

Buchan, K.L., Ernst, R.E., 2004. Diabase dyke swarms and related units in Canada and adjacent regions. Geological Survey of Canada, Map 2022A (scale 1: 5,000,000) and Accompanying Notes.

Connelly, J.N., van Gool, J.A.M., Mengel, F.C., 2000. Temporal evolution of a deeply eroded orogen: the Nagssugtoqidian Orogen, West Greenland. Can. J. Earth Sci. 37, 1121–1142.

Escher, J.C., Pulvertaft, T.C.R., 1995. Geological map of Greenland 1: 2 500 000. Copenhagen: Geol. Surv. Greenland.

Hall, R.P., Hughes, D.J., 1987. Noritic dykes of southern Greenland: early Proterozoic boninitic magmatism. Contrib. Mineral. Petrol. 97, 169–182.

Kalsbeek, F., Taylor, P.N., 1985: Age and origin of early Proterozoic dolerite dykes in South-West Greenland. Contrib. Mineral. Petrol. 89, 307–316.

Nilsson, K.M.M., Söderlund, U., Ernst, R.E., Hamilton, M.A., Scherstén, A., Armitage, P.E.B, 2010. Precise U-Pb baddeleyite ages of mafic dykes and intrusions in southern West Greenland and implications for a possible reconstruction with the Superior craton, Precambrian Res., in press.

Nutman, A.P., Kalsbeek, F., Marker, M., van Gool, J., Bridgwater, D., 1999. U-Pb zircon ages of Kangâmiut dykes and detrital zircons in metasediments in the Palaeoproterozoic Nagssugtoqidian Orogen (West Greenland); clues to the pre-collisional history of the orogen. Precambrian Res. 93, 87–104.

Nutman, A.P., Kalsbeek, F., Friend, C.R.L., 2008. The Nagssugtoqidian orogen in South-East Greenland: Evidence for Paleoproterozoic collision and plate assembly. American J. Sci., 308, 529–572, doi:10.2475/04.2008.06

Söderlund, U., Hofmann, A., Klausen, M. B., Olsson, J.R., Ernst, R.E., 2010. Towards a complete magmatic barcode for the Zimbabwe craton: Baddeleyite U-Pb dating of regional dolerite dike swarms and sill complexes. Precambrian Res., in press, doi:10.1016/j.precamres.2009.11.001.

Willigers, B.J.A., Mengel, F.C., Bridgwater, D., Wijbrans, J.R., van Gool, J.A.M., 1999. Mafic dike swarms as absolute time markers in high-grade terranes: $^{40}Ar/^{39}Ar$ geochronological constraints on the Kangâmiut dikes, West Greenland. *Geology 27*, 775–778.

Field observations, whole rock chemistry and combined zircon U/Pb/Hf/O isotope analyses from the Ilivertalik Augen Granite, southern West Greenland: Evidences for an igneous granite - charnockite relationship

Tomas Næraa[1,2], Anders Scherstén[3] and Thomas F. Kokfelt[1]

[1)] *Geological Survey of Denmark and Greenland (GEUS), Denmark.*
[2)] *Natural History Museum of Denmark, Copenhagen University, Denmark.*
[3)] *Department of Geology, Lund University, Sweden.*

Introduction

The Tasiusarsuaq high grade gneiss terrane is composed of mainly TTG gneisses with intrusive ages ranging from ca. 3.3 to 2.8 Ga (Næraa and Scherstén 2008 and GEUS internal data). Subordinate greenstones are intercalated with the gneisses, generally with tectonised boundaries. Except for Nunatak 1390, the greenstones are integrated in the gneiss terrane and not associated with terrane boundaries (Scherstén et al. 2008).

Granulite facies is preserved in a large part of the terrane, the remaining part of the terrane is in amphibolite facies, which might be of either retrograde or prograde origin (e.g. Windley & Garde, 2009; McGregor et al., 1991). The Ilivertalik Augen Granite (IAG) is partly charnockitic (orthopyroxene-bearing) in nature, and it has been suggested that IAG intruded under granulite facies conditions (Pidgeon and Kalsbeek 1978), which is confirmed by our field observations.

Here we present field observations, whole rock major and trace element chemistry and combined zircon U/Pb/Hf/O isotope data from a number of widely spaced localities within the IAG. We focus our discussion on the igneous relationship between granite and charnockite and on the nature of the protolith.

Results

The studied samples from the IAG are feldspar phenocrystic, have SiO_2 contents ranging from 58 to 73 wt%, and classify as granodiorites and granites (O'Connor, 1965). Whole rock contents of MgO, $Fe_2O_{3(total)}$, CaO and TiO_2 show negative correlation with SiO_2, and K_2O correlates positively with SiO_2.

Several of the samples are orthopyroxene-bearing and we classify these as charnockitic granodiorites. The whole rock geochemistry is reflected in the mineralogy, as samples with high Fe and Mg generally contain igneous orthopyroxene. In the field we have observed transitions from charnockitic granodiorite to granodiorite occurring on a meter scale (see Fig. 1).

Figure 1. *Field relation showing transition from charnockitic granodiorite to granodiorite.*

Zircon U/Pb ages have been obtained from five rocks with granitic and charnockitic mineralogy. Each sample has well defined igneous zircon population and the weighted mean $^{207}Pb/^{206}Pb$ age of the five samples range 2793±3 to 2799±2 Ma. The sample with the lowest age shows ancient Pb-loss with ages tailing off towards 2.7 Ga and with a negative correlation between U concentration and age.

Combined zircon U/Pb/Hf/O isotope data have been obtained from a charnockitic granodiorite, a granodiorite and a granite (senso stricto) from the northern part of the IAG. The sample have a similar hafnium isotope composition ranging from ca. +1 to -1 $\varepsilon Hf_{(t)}$ units (Fig. 2). Oxygen isotope compositions analysed in zircons from three different samples show a restricted variation with weighted mean $\delta^{18}O$ values of the three samples of 6.25±0.28, 6.25±0.28 and 6.61±0.16 ‰ (values relative to SMOW and errors reflecting the 2σ level). Thus, taking the analytical errors into account, the analysed samples are indistinguishable both with respect to $\varepsilon Hf_{(t)}$ and $\delta^{18}O$.

Discussion and Summary

Whole rock major element chemistry of the IAG show a negative correlation of MgO, $Fe_2O_{3(total)}$, CaO and TiO_2 relative to SiO_2 and the samples with a larger mafic component are orthopyroxene-bearing. The five dated samples are from widely spaced localities within the IAG, and they include both orthopyroxene-bearing and orthopyroxene-free varieties, where orthopyroxene is prevalent in the more mafic compositions as an igneous phase. All samples yield statistically contemporaneous igneous ages, with a weighted mean $^{207}Pb/^{206}Pb$ age of 2797±3 Ma. The hafnium isotope composition of the IAG is homogeneous with $\varepsilon Hf_{(t)}$ values ranging from +1 to -1. Likewise oxygen isotope compositions are homogeneous with mean $\delta^{18}O$ values of the individual samples ranging from 6.25±0.28 to 6.61±0.16 ‰.

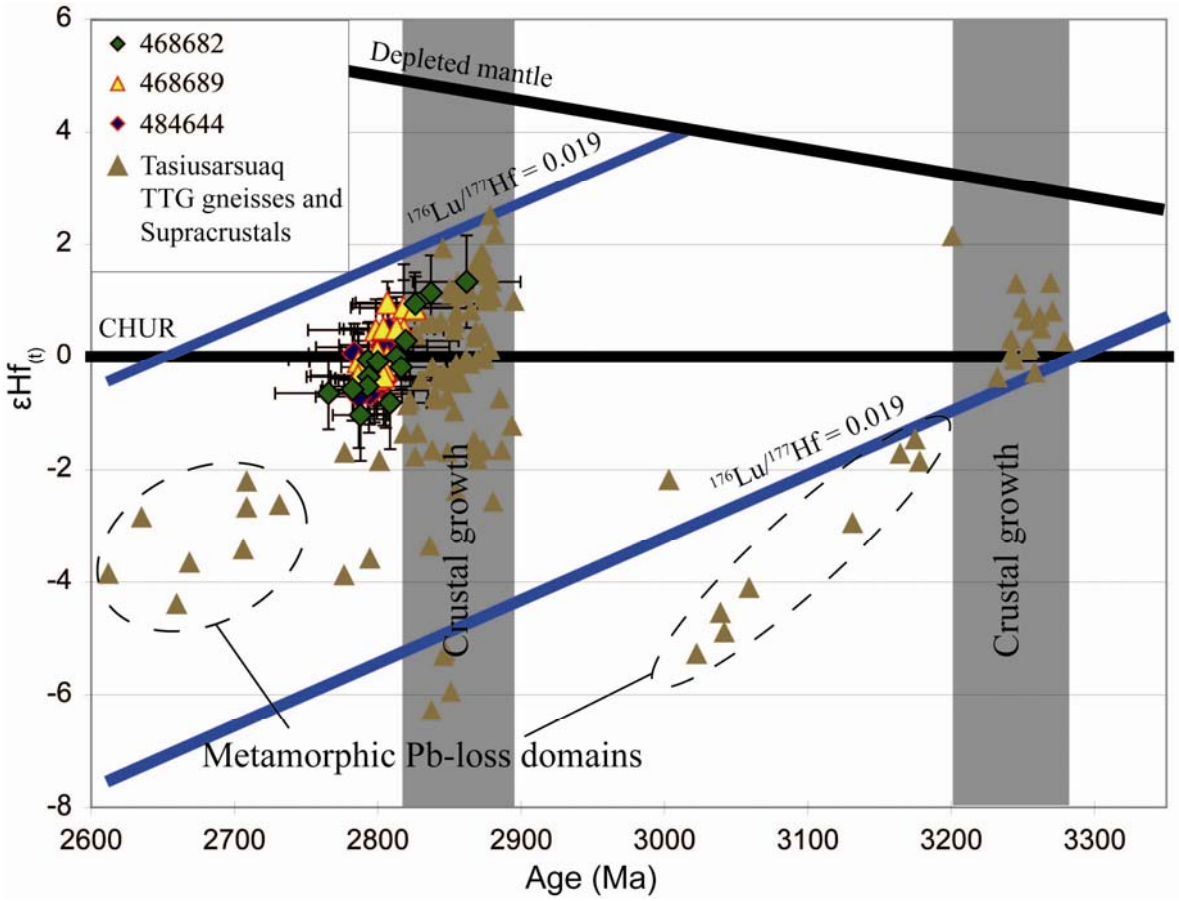

Figure 2. *$\varepsilon Hf_{(t)}$ versus age diagram. Ilivertalik augen granite (sample 468682, 468689 and 484644) plotted together with unpublished data from Tasiusarsuaq TTG gneisses and supracrustal rocks from Nunatak 1390. The grey areas represent crystallisation ages. Blue lines are added to indicate the Hf isotope development in an average crust composition. Depleted mantle from Pietranik et al. (2009).*

The contemporaneous ages and isotopic homogeneity in the samples suggest that an igneous relationship is likely to exist between the orthopyroxene-bearing and orthopyroxene-free parts of the IAG, and that the presence of igneous orthopyroxene is principally determined by whole rock chemistry (including the partial water pressure of the magma).

The hafnium isotope composition of the depleted mantle at the time of the intrusion of the IAG is constrained from ca. 2.88 Ga TTG gneisses and a supracrustal unit of the Tasiusarsuaq terrane that have $\varepsilon Hf_{(t)}$ values up to ca +2 (Næraa and Scherstén unpublished data) (Fig.2). World wide data suggest that the depleted mantle have $\varepsilon Hf_{(t)}$ values of ca +4 at 2.8 Ga (Hawkesworth et al., 2010). The observed hafnium isotope composition from the IAG at -1 – +1 $\varepsilon Hf_{(t)}$ units therefore does not suggest any pronounced mantle input into the crust during the melting event. Furthermore, the homogeneous $\varepsilon Hf_{(t)}$ values from the analysed samples does not imply mixing between different crustal reservoirs. We therefore suggest that the IAG was formed by remelting of a homogeneous crustal reservoir that relates to the formation of the younger ca. 2.90 to 2.84 Ga TTG crust of the Tasiusarsuaq terrane.

References

Hawkesworth, C.J., Dhuime, B, Pietranik, A.B., Cawood, P.A., Kemp, A.I.S. & Storey C.D. (2010). The generation and evolution of the continental crust. Journal of the Geological Society, London, 167, 229–248.

McGregor, V.R., Friend, C.R.L. & Nutman, A.P. (1991). The late Archaean mobile belt through Godthåbsfjord, southern West Greenland: a continent–continent collision zone? Bulletin of the Geological Society of Denmark 39, 179–197.

Næraa, T. & Scherstén, A. (2008). New zircon ages from the Tasiusarsuaq terrane, southern West Greenland. Geological Survey of Denmark and Greenland Bulletin 15, 73–76.

O'Connor, J.T. 1965. A classification for quartz-rich igneous rocks based on feldspar ratios. In: US Geological Survey Professional Paper B525. USGS, 79–84.

Pidgeon, P.T. & Kalsbeek, F. (1978). Dating of igneous and metamorphic events in the Fiskenæsset region of southern West Greenland. Can, J. Earth. Sci., 15, 2021-2025.

Pietranik, A.B., Hawkesworth, C.J., Storey, C. & Kemp, T. (2009). Depleted mantle evolution and how it is recorded in zircon. Geochimica et Cosmochimica Acta, 73, A1028.

Scherstén. A, Stendal, H. & Næraa, T. (2008). Geochemistry of greenstones in the Tasiusarsuaq terrane, southern West Greenland. Geological Survey of Denmark and Greenland Bulletin 15, 69-72.

Windley, B.F. & Garde, A.A. 2009. Arc-generated blocks with crustal sections in the North Atlantic craton of West Greenland: Crustal growth in the Archean with modern analogues. Earth-Science Reviews 93, 1–30.

Digital field data capture in Greenland: GanFeld news

Denis Martin Schlatter, Uffe Larsen & Bo Møller Stensgaard

The Geological Survey of Denmark and Greenland (GEUS) has developed in cooperation with the Geological Survey of Canada (GSC) a digital field data capture system in the spring of 2008 (Buller 2002, 2004, 2005). In the summers of 2008 and 2009 GEUS has carried out a field based test of this system in South Greenland (Schlatter & Larsen 2009; Schlatter *et al.* 2010). During this field test several hundred field localities were described by using the digital field data capture system (hereafter referred to as "GanFeld"). In the summer of 2009, GanFeld was used not only for the southern West Greenland expedition, but also for the South East Greenland expedition where one of the main focuses was a large regional sediment sampling program.

Here we want to discuss the most important improvements of GanFeld such as the addition of a new module capable to capture digitally field data related to sediment samples and a function which makes it possible to backup the digital field data while doing field work.

Equipment and concept

As GEUS is working in remote areas, often with access to the outcrops only by foot, it became apparent that lightweight PDAs are more convenient to use than larger and weighty tablet PCs.

Each digital field data capture system used by GEUS comprises a HP iPAQ 214 Entreprise Handheld PDA (Fig. 1a), a wireless GPS (Fig. 1b), a spare battery (Fig 1c), two replacement stylus pens (Fig. 1 d) and a spare secure digital (SD) memory card (Fig. 1e).

Figure 1. *The digital field data capture system consists of: a) HP iPAQ PDA (310 €); b) wireless GPS receiver (48 €); c) HP extended battery (59 €); d) PDA stylus (7 € for each stylus); e) secure digital (SD) memory card (15 €).*

Power for the PDA and the GPS receiver are supplied by solar energised power generator or petrol engine generator.

Field work accomplished by a geologist usually comprises a sequence of activities that are carried out in a similar way at each outcrop (earth material). Such a sequence normally starts by the determination of the geographic location using a GPS receiver. Once the position is recorded, the rock type is determined and described, and then other information such as structural measurements on the outcrop is taken. Bedrock samples are collected and described and, photographs are taken and annotated for documentation. Additionally, stream, soil, or scree sediment samples are collected. GanFeld allows capture of field data systematically in an organised and modular manner. Table 1 summarises the type of information that is digitally captured while performing field work.

Module:	Page number:	Pages:
"Station"	1	Coordinates (provided via GPS in three different coordinate systems)
	2	Elevation; observation type; team partner; camp ID
	3	Station "short note"; since last station "short note"; "large note"
"Earth Material"	1	Rock class; rock type; rock name; colour
	2	Minerals; abundance and size of minerals; metamorphic facies
	3	Alteration; ore minerals; abundance and size of minerals
	4	Textures (three different textures can be captured)
	5	Lithological map unit; "short notes" for material description; "large notes"
	6	Chronostratigraphy; era, period, epoch
	7	Fossils
"Rock Sample"	1	Sample type; purpose; GEUS sample number
	2	Sample orientation; sample depth, "short notes", "large notes"
"Structure"	1	Class; type; detail
	2	Method (right hand rule or dip dip direction); Azimuth and dip measurement
	3	"Short notes"; "large notes"
"Photo"	1	Category; File ID from digital camera; direction of picture; time of picture
	2	Photo caption (possibility to load previous caption); "large note"
"Sediment sample"	1	Stream Sediment (sub-module with 4 pages)
	2	Soil Sediment (sub-module with 3 pages)
	3	Scree Sediment (sub-module with 3 pages)

Table 1. *Field data are captured using the six GanFeld modules: "Station", "Earth Material", "Rock sample", "Structure", "Photo" and "Sediment sample" and each of these modules consists of two to seven pages. (Note: "short notes" refer to text string up to 254 characters and "large notes" to text entry of unlimited length).*

An earth material for example is captured by tapping the hammer icon in the menu bar (Fig. 2a). This activates the window where the details of the earth material can be registered by using predefined drop-down lists for an accurate rock description (Fig. 2b) whereas minerals are selected one after the other from a different drop-down list (Fig. 2c).

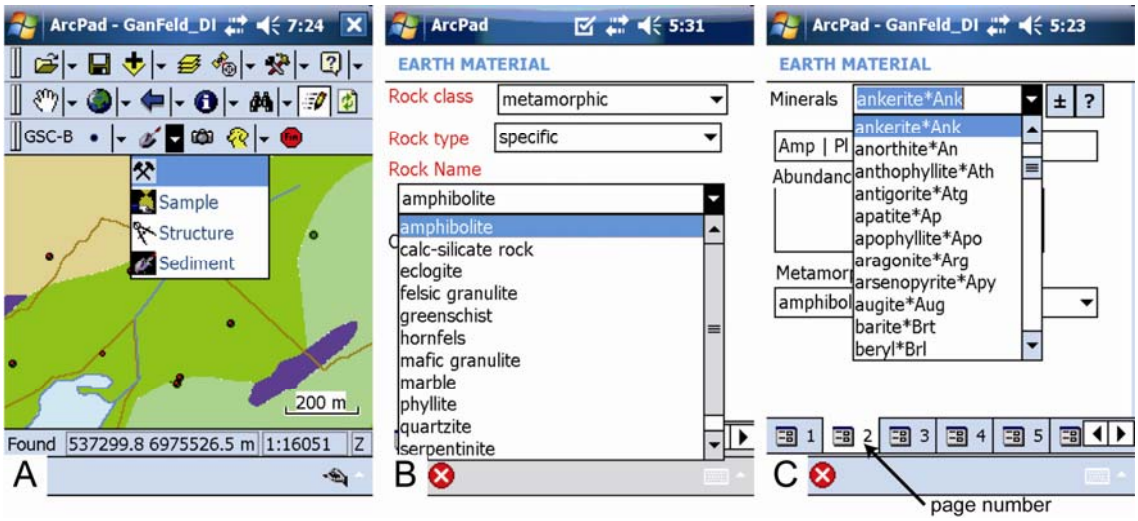

Figure 2. *Sequence of digital field data capture for "Earth Material": a) a small hammer icon is activated to capture the field data seen at an outcrop. Other icons are sample bag (for samples), compasses (for structures) and shovel (for sediment samples). The location of the outcrop has already been captured previously and corresponds to one of the small dots on the geological map; b) the field data of the earth material is captured; c) the minerals identified at the outcrop are captured using the drop-down list with predefined minerals. Several minerals can be selected one by one and are concatenated into a series or string of words in a combo box.*

GanFeld allows geologists to capture information in a consistent manner in which predefined classifications and descriptions are used resulting in a consistent description of localities and geology amongst geologists. GanFeld also guides the geologist through a step by step process to ensure that all necessary rock outcrop description information, following GEUS standards for Greenland, is captured. Base layers as for example a digital geological vector map (Fig. 2a) can easily be added and displayed directly on the screen of the PDA (Schlatter & Larsen 2010). Individual geologists can add and remove maps by attaching the PDA to a computer or by simply storing maps as shape files or georeferenced tiff-image files on the SD memory card which is part of the field capture system (Fig. 1e).

Module for sediment sampling

Figure 3 shows how the recently by GEUS programmed module for sediment sampling is structured. One of three sample types can be selected: stream sediment, soil sediment or scree sediment (Figure 3a).

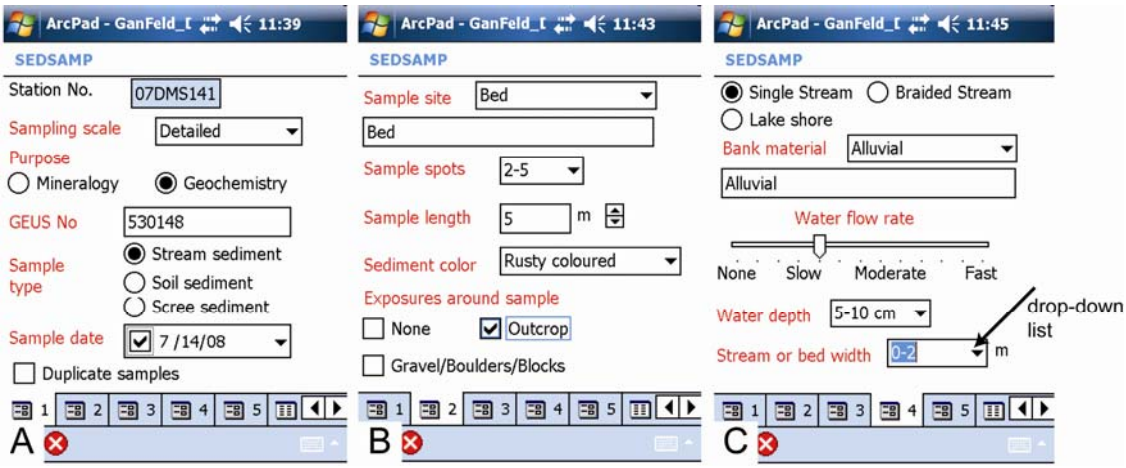

Figure 3. *Sequence of digital field data capture for "Sediment sample": a) three types of sediment samples can be captured: stream, soil and scree sediment samples; b) the sample site and sample is described by using drop-down lists which are activated by clicking inside the small black arrows (on the right side of the combo boxes); c) the stream from which the sample is taken is described. The water flow rate is characterised by using a scale bar.*

Several drop-down lists within the sediment sample form (Figs 3b and 3c) facilitates the field data capture with little free text being entered which makes the procedure of field data capture for sediment samples fast and efficient.

Backup

Regular backups of the digital field data are essential. This can be done while carrying out field work by clicking on the icon "Backup" which is located on the right hand of the lowest menu bar (Fig. 4a).

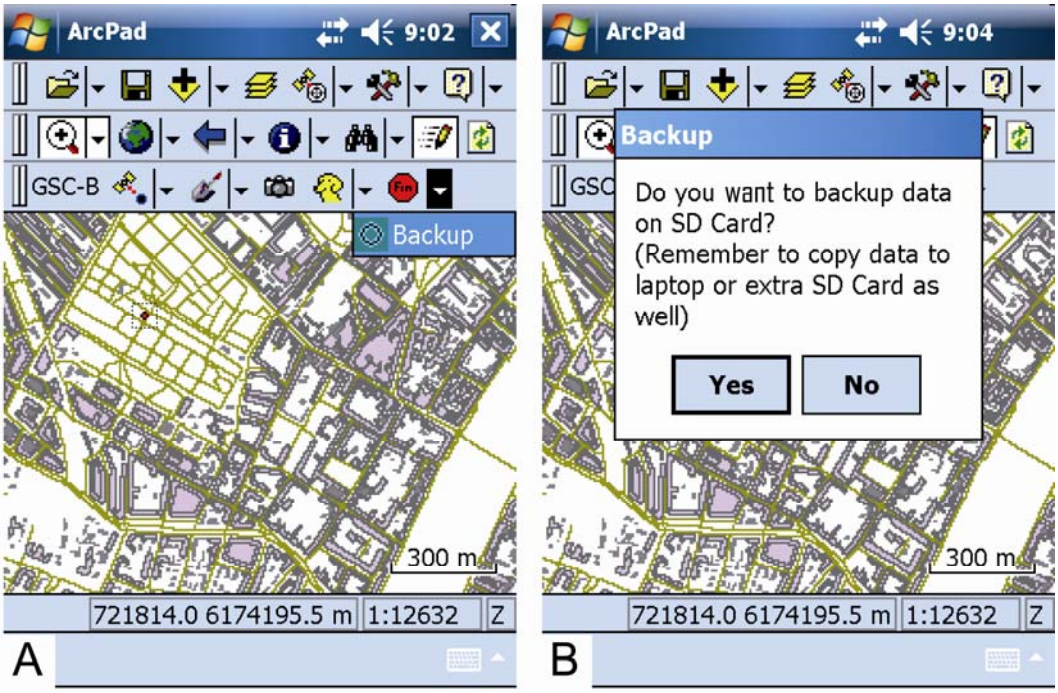

Figure 4. *The screen shot shows how the backup feature of the GanFeld works. Simply click "Yes" and your GanFeld data will be stored. (The base layer chosen for this example is the map of Copenhagen; and the station shown is located in the King's Gardens which is the country's oldest royal garden).*

Once the "Backup" icon is tapped, a new dialog box appears where you can authorise the system to back up your data on the SD memory card (Fig. 4b). GanFeld is programmed in a way that the user is prompted to make a backup after every 6 hours. In detail the GanFeld data are stored under the path "My Device\My Documents" as default in the internal memory of the PDA. Because this internal memory is not protected in the case of a major break down of the PDA; it is important that the data are also stored as a backup on the SD memory card as described above. (The interested reader is referred to the GEUS internal field manual "Field instructions and Standards 2010" to read in detail how the GanFeld data are copied onto the SD memory by creating a folder for each day). It is of course important to copy the GanFeld data also on your laptop or on an extra SD memory card on a daily basis; because of the risk of the loss of a PDA.

The digital field data from the field teams normally are sent to the base camp on SD memory cards on a regular basis. This allows the base camp to compile and analyse all captured data. The visited outcrops are plotted on a geological map which provides the possibility of verifying the quality of the information and the progress of the field work. Geologists at base camp can interpret the data while in the field and plan field activities accordingly. Furthermore, digital field data can easily be shared at the end of the field season. If the base camp does not have the capacity to compile the data of all the field teams, the project leaders are responsible that the GanFeld data of their field teams are properly stored.

Reporting of field data

One of the largest advantages of the use of digital field data capture for GEUS is a faster reporting of the data of each field season because the field data are already digitally avail-

able and geologists do not need to spend time entering data manually into spreadsheets from field diaries which is not only time consuming but can introduce errors. For this, a reporting facility is being developed as a web accessible error checking and editing tool which also enables the production of a standard report in a PDF format that contains all digitally captured field data for each station.

Conclusions and outlook

In summary, since digital field data capture has been introduced at GEUS with the use of PDAs and GanFeld, field data are neatly organised and reporting and sharing of data has become easier. The past experience has also shown that it was relatively easy to add new functions important to GEUS onto GanFeld, such as for example a module to capture sediment samples and a safe backup routine. The system can be developed in the future so that existing data within GEUS databases can be plotted in the GanFeld system, for example existing lithogeochemical data of an area. The GanFeld system will be developed further by adding new modules which are able to capture other types of field data, such as geochemical, petrophysical and geophysical data.

Acknowledgements

Our thanks to the GSC for helping GEUS to implement the digital field data capture at GEUS and for allowing GEUS to use the GanFeld software.

References

Buller, G. 2002: Capturing Digital Data in the Field - Ganfield: data integrity from field to final product. Workshop, British Geological Survey, Nottingham, England 25 & 26 April 2002.

Buller, G. 2004: GanFeld: Geological Field Data Capture. U.S. Geological Survey Open-File Report **2004–1451**, 49-53.

Buller, G. 2005: A conceptual approach to the development of digital geological field data collection. Open File Report U S Geological Survey, Report # OF, **2005-1428**, 91-96.

Schlatter, D.M. & Larsen, U. 2009: GanFeld: introduction and news. In: Kolb J. & Kokfelt T. (eds). Annual workshop on the geology of southern West Greenland related to field work: abstract volume 1, Danmarks og Grønlands Geologiske Undersøgelse Rapport **2009/21**, 22-23.

Schlatter, D.M. & Larsen, U. 2010: Using digital field data capturing in Greenland: Experience from 2008/9 GEUS field seasons. In: NAKREM H.A., HARSTAD A.O. & HAUKDAL G. (eds). 29th Nordic Geological Winter Meeting. Geological Society of Norway, 173-174.

Schlatter D.M., Buller G., Larsen, U. & Møller Stensgaard B. 2010: Digital field data capture: the Geological Survey of Denmark and Greenland experiences in Greenland. Explore No. 147 (in press).

Pressure and temperature constraints on metamorphism of and the P-T trajectory for altered volcanic rocks from Qilanngaarsuit Island, east of Qarajat Iluat fjord and Ikkattup Nunaa

John C. Schumacher[1], Charlotte Stamper[1], Gemma Sherwood[1], Nynke Keulen[2], Sandra Piazolo[3]

[1]*Dept. of Earth Sciences, Wills Memorial Building' Queen's Road, Bristol, BS8 1RJ, United Kingdom*

[2]*Geological Survey of Denmark and Greenland, Øster Voldgade 10, DK-1350 Copenhagen K, Denmark*

[3]*Dept. of Earth and Planetary Sciences, Macquarie University, Sydney, NSW 2109, Australia*

This study focuses on the stages of metamorphism recorded in volcanic rocks that underwent high temperature hydrothermal alteration by seawater prior to metamorphism. The net geochemical effect on the rocks that have undergone this type of alteration is to remove Ca and to a lesser extent Na at the same time increasing the Mg in the rock. These chemical changes are manifested by breakdown of plagioclase and the plagioclase component in volcanic glass, and the growth of chlorite, in part from Mg in seawater. In southern West Greenland these rock compositions, where large enough to be shown at the map scale of the geologic maps, are commonly shown as metasediments. Three localities were studied: Qilanngaarsuit Island (63° 51.465'N, 51° 38.908'W, locality 1), locality 2 is east of the small Qarajat Iluat fjord (63° 58.521' N, 51° 18.006'W) and locality 3 at Ikkattup Nunaa (62° 40.855'N, 50° 12.130'W). Localities 1 and 2 are in the Færingehavn and Tre Brødre terranes of (Friend et al. 1987), respectively, and both are located in the northern part of the 62 V1N Buksefjord 100K map sheet. Locality 3 is on the 63 V1N Bjørnesund 100K map sheet.

Mineralogy and Assemblages

These rocks are highly variable in composition and the observed assemblages consist of various combinations of the following minerals: sillimanite, kyanite, staurolite, Al-spinel, cordierite, garnet, chlorite, orthoamphibole, biotite, corundum, quartz and plagioclase. Accessory minerals include: apatite, allanite, monazite, xenotime, zircon, rutile and ilmenite. Mineral assemblages at localities 1 and 2 are similar, and they differ from the mineral assemblages at locality 3. The significant differences are: (a) no cordierite is found at locality 3; (b) no aluminosilicate was found at locality 3; (c) the orthoamphiboles at localities 1 and 2 show a continuum of compositions from high to low aluminum content, while the orthoamphiboles at locality 3 cluster at discrete high or low aluminum contents. These differences could be due to variations in metamorphic grade, to slight variation in bulk composition or both. At all three localities, layers of amphibolite ± garnet are also present.

Reaction Textures

The cordierite-bearing rocks at localities 1 and 2 give the clearest indication of P-T trajectory. At locality 2, texturally early kyanite that is partly replaced by sillimanite was found in one sample. The aluminosilicate in the sample continued to react with quartz and orthoamphibole to form cordierite. Cordierite stability is pressure sensitive and its presence as rims

on either garnet or sillimanite demonstrates texturally later cordierite growth and suggests a general clockwise P-T trajectory near the peak metamorphic conditions.

P-T estimates

At all three localities, a variety of methods were used to estimate temperature and pressure. These included using thermodynamic databases to locate the P-T conditions of observed mineral assemblages (Connolly 2005), various traditional geothermometers and geobarometers and locations of limiting reactions in P-T space. Both localities 1 and 2 suggest maximum temperatures of 600-650°C based on the T ranges of observed assemblages. These P-T estimates are consistent with minimum temperatures suggested by the orthoamphiboles (Fig. 1). The orthoamphiboles from these rocks span the range of compositions from anthophyllite to gedrite, which suggests the orthoamphiboles crystallised above the peak of the orthorhombic-amphibole solvus and gives a minimum metamorphic peak temperature of about 600°C. The presence of amphibolites suggests upper amphibolite-facies conditions and temperatures below about 700°C.

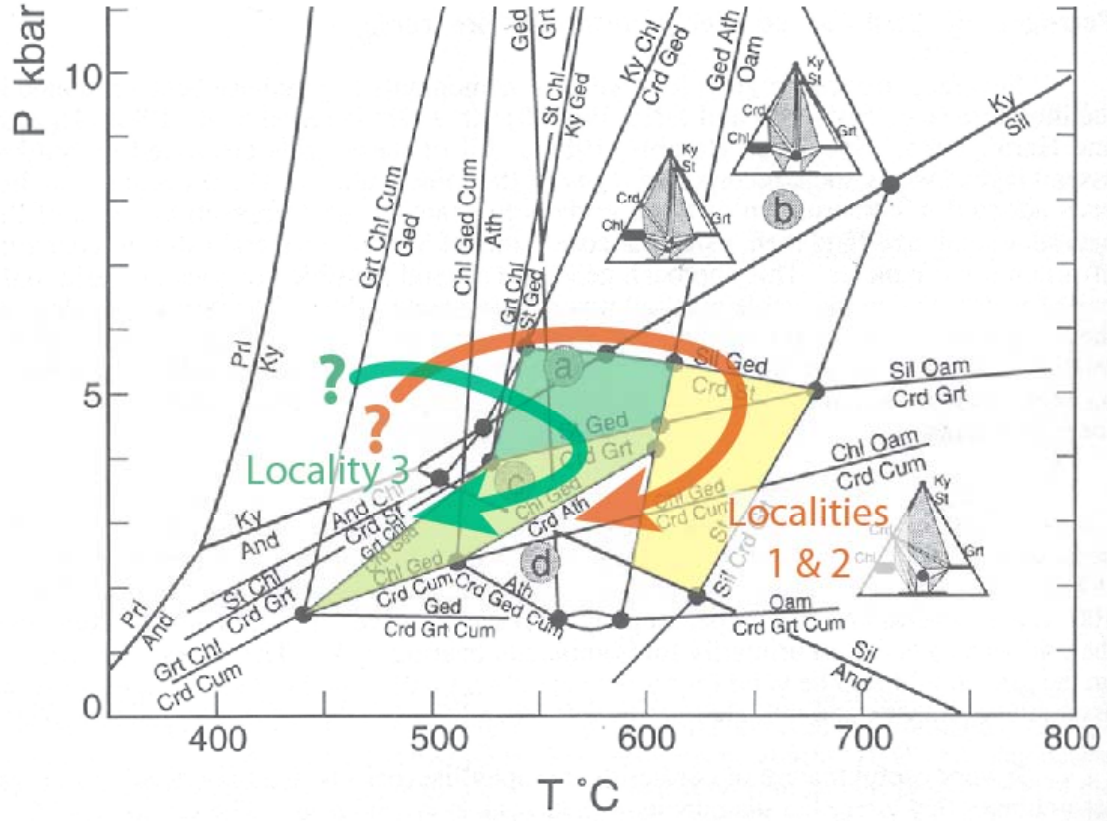

Figure 1. *P-T diagram that shows univariant Fe-Mg reactions for rocks with bulk compositions derived from hydrothermally-altered volcanic rocks (from Spear 1993). Yellow yield: metamorphic conditions for localities 1 and 2. Green shaded fields: peak and retrograde metamorphic conditions from locality 3.*

The assemblages at locality 3 suggest lower peak temperatures. No cordierite or aluminosilicate phase is found, and staurolite is the most common Al-rich mineral in most locality-3 rocks. The assemblages also suggest that these rocks are generally richer in Fe than those at localities 1 and 2. In one of the rare Mg-rich bulk compositions at locality 3, orthorhombic amphibole and chlorite are stable; these minerals together with the absence of cordierite support lower peak temperatures. The P-T estimates using mineral compositions and equilibria calculated with PerPlex_X (Connolly 2005) and conventional geothermobarometry suggest maximum T of about 480-550°C and P below 5 kbar (Fig. 1). The lack of ranges of Al contents in the orthoamphibole together with the restriction of Al contents in orthoamphibole to either low or high values suggests that orthoamphibole formation at temperatures that lie below the 600°C crest of the orthoamphibole solvus. We have also attempted to date metamorphic monazite at locality 3 where textures show that the monazite crystallised in the metamorphic assemblage. The cores of this monazite give an age of metamorphism of about 2.7 Ga.

Summary

The P-T is broadly constrained in these rocks by the stability of staurolite + quartz, the orthoamphibole solvus and the presence of amphibolites ± garnet at all localities. The presence of staurolite in these rock types seems a reliable indicator of peak metamorphic conditions which do not exceed the amphibolite to upper-amphibolite facies. The P-T trajectories appear to be clockwise and suggest a phase of geologically rapid uplift at or around the time of maximum T (about 2.7 Ga).

References

Connolly, JAD 2005. "Computation of phase equilibria by linear programming: A tool for geodynamic modeling and its application to subduction zone decarbonation." *Earth and Planetary Science Letters* **236(1-2)**: 524-541.

Friend CRL, Nutman AP & McGregor VR 1987. Late-Archaean tectonics in the Færingehavn – Tre Brødre area, south of Buksefjorden, southern West Greenland. *J. Geol. Soc. Lond.* **144**, 369–376.

Spear, FS 1993. Metamorphic Phase Equilibria and Pressure-Temperature-Time Paths. Monograph Series, Washington, D. C., Mineralogical Society of America, 799 p.

Supracrustal rocks of the Tartoq Group, SW Greenland

Kristoffer Szilas

During the 2009 field work in the Tartoq area a total of 112 samples were collected by Brian Windley, Vincent van Hinsberg and myself. The rocks were analysed for major and trace elements at ACME labs in Vancouver, and 62 polished thin sections were prepared by GeoTech Labs also located in Vancouver.

The rocks have experienced greenschist facies metamorphic conditions, so all lithologies should have the prefix 'meta', which is omitted here for simplicity. Chlorite is present in all samples, which together with their fine grain size can make field identification difficult. On the basis of field descriptions, geochemistry and petrography the rocks have been classified into a number of groups and they will be described below, which includes the following lithologies: marble, bedded chert, qz-sediment, mudrock and greenschist.
The samples were collected from three different areas in the Tartoq area with the majority coming from the Nuuluk supracrustal belt (Fig. 1).

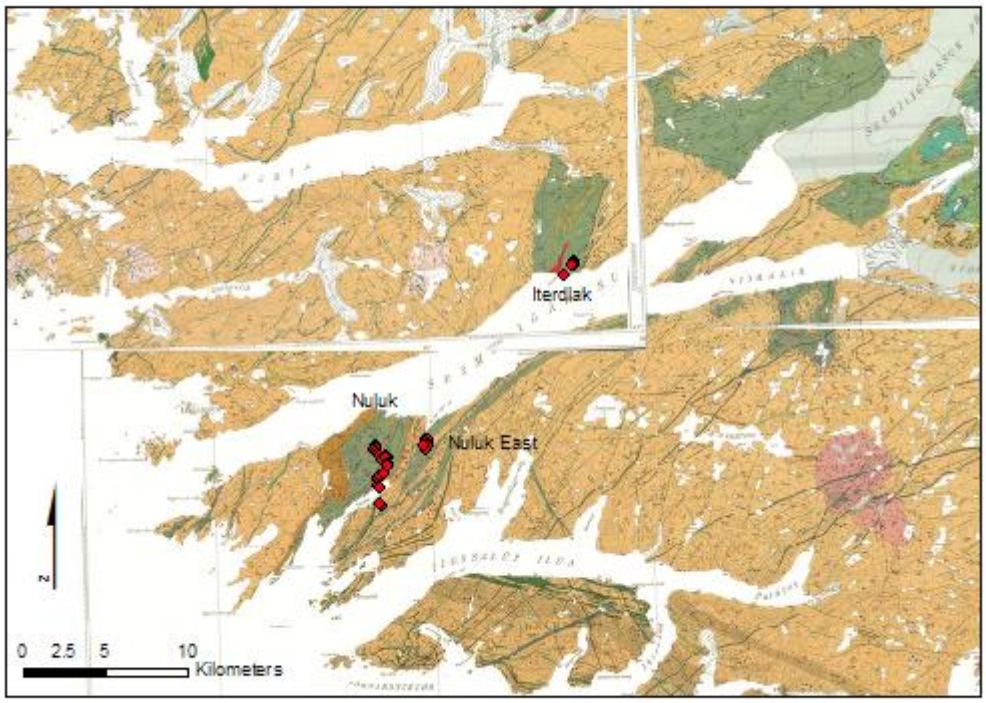

Figure 1. *Map showing sample localities in the Tartoq group from the 2009 field season.*

Lithologies

Marbles were found at Nuuluk (510869) and Nuuluk East (510852) as meter wide beds of qz-laminated carbonate rocks. These units can be traced for several km along strike and are folded together with the greenschist rocks surrounding them.

Bedded chert is located in the central part of Nuuluk (510893) and forms a few meters wide unit. This rock is finely laminated, showing cross bedding and some parts have sulfide replacement.
Qz-sediments can be difficult to identify, as mention above, because of the generally fine grain size and pervasive chlorite impregnation. However, at Nuuluk East some proper sandstones (e.g. 510853) were found that had well-rounded qz-grains supported in a matrix of carbonate. The fine grained variety is generally laminated and in thin section they have alternating layers of qz and white mica.
Mudrocks (e.g. 512253) are almost impossible to identify in the field and is likely a group of rocks that represent a transition from greenschists to qz-sediments in terms of sedimentary maturity. Thus they vary in appearance from that of cherts to laminated greenschists.
Greenschists are by far the dominating lithology in the supracrustal belts of Tartoq and are characterised by high chlorite content and generally fine grain size. They range from massive rocks with ophitic texture (512283) to nobly carbonate-rich schist (510895).

Geochemistry

The marbles may represent chemical sediments and have trace element-patterns that are similar to their surrounding lithologies indicating syn-deposition and derivation of their silisic lamina from the immediate vicinity. Their SiO_2 content is around 40 wt-% and the samples from Nuuluk and Nuuluk East plot towards ankerite and dolomite end members, respectively.
Interestingly, the bedded cherts have trace element patterns and concentrations similar to the greenschists and even their major element content is relatively similar (Fig. 2). Additional work by XRD and electron microprobe is planned to establish the origin of this unit.

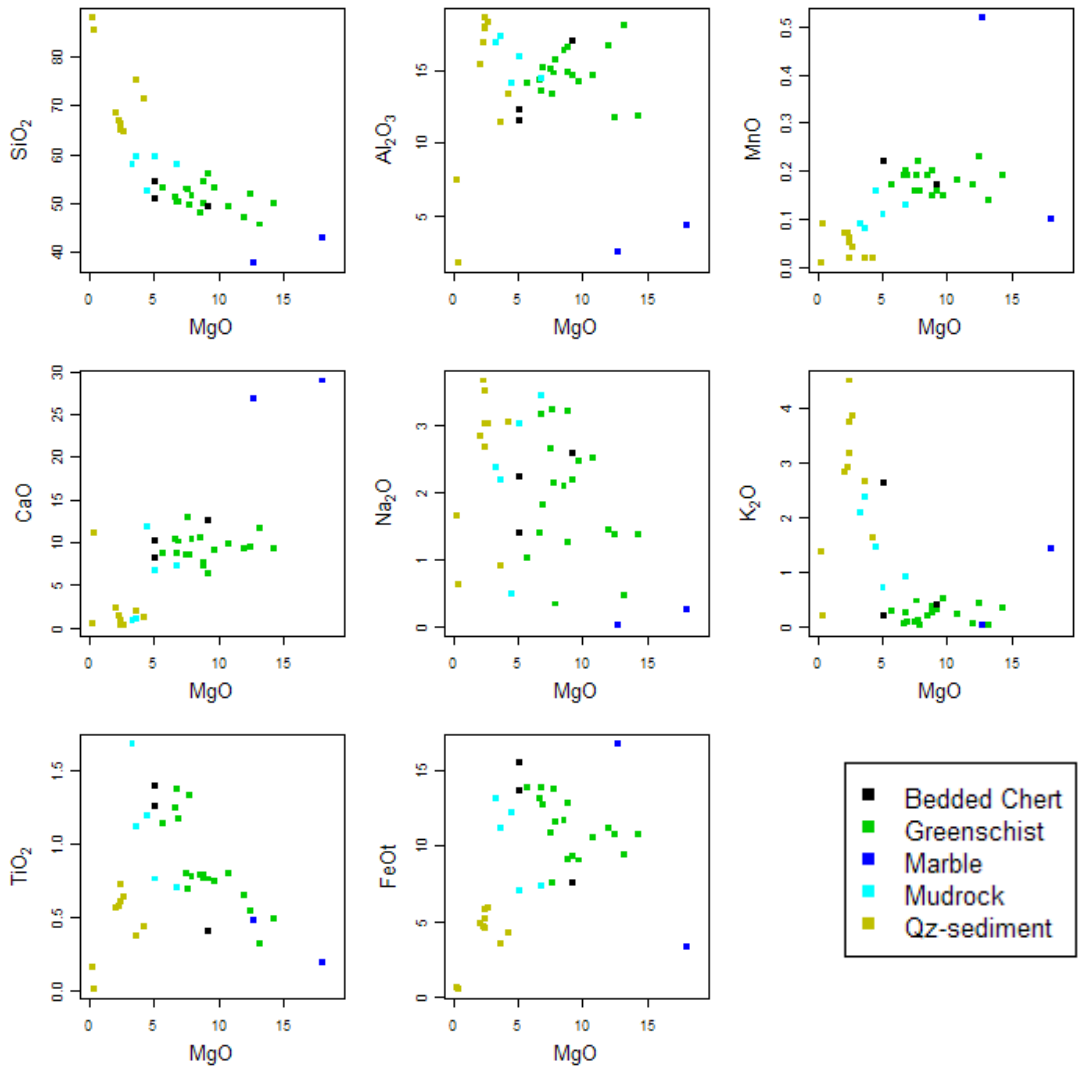

Figure 2. *Major element plots against MgO for all of the supracrustal lithologies collected in Tartoq.*

The mudrocks have been classified primarily based on their REE-patterns with a La_N/Sm_N ratio of about 3 and SiO_2 content between 50-60 wt-%. This group of rocks can probably only be defined from geochemical data and have distinct negative Nb-Ta anomalies that indicate derivation, at least in part, from an enriched crustal source (Fig. 3). Their major and trace element abundances generally lie between those of the greenschists and the qz-sediments, which indicates mixing of these two sources or some intermediate stage of sedimentary maturity.

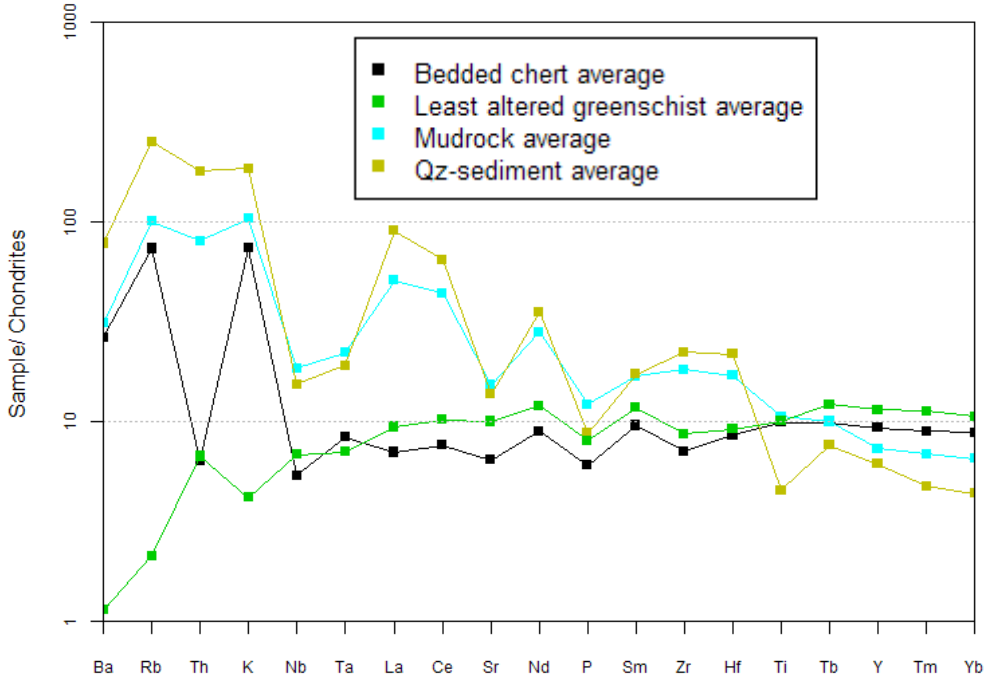

Figure 3. *Chondrite-normalised trace element diagram.*

All Qz-sediments have SiO_2 contents above 60 wt-% and have steep REE-patterns with La_N/Sm_N ratios around 5, as well as negative Nb-Ta-Ti anomalies, indicating a derivation from a crustal source similar to what is observed for the mudrocks, only even more enriched as seen from the steeper REE-pattern.

The greenschists form a group that scatter heavily on binary element plots. This together with diverse textures ranging from ophitic (consistent with volcanic flow) to layering and fine lamination suggests that some of the geochemical variation is caused by transportation, weathering and alteration processes. The readily recognizable indications of alteration, such as qz- and carbonate veining together with a peraluminous geochemistry, are used to identify the freshest greenschists, as these rocks might reveal information about their volcanic origin. Out of 55 samples classified as greenschists only 18 were without visible traces of alteration and out of these only 5 had relict cpx and igneous texture that was unequivocal evidence for a magmatic rather than sedimentary origin. Thus, it seems likely that the majority of the greenschists are epiclastic rocks that represent some degree of reworking of volcanic material by sedimentary processes.

The screened 'least altered' samples classify as tholeiitic basalts, and show a characteristic depleted chondrite-normalised trace element pattern consistent with a MORB or an island arc tholeiitic affinity. The supracrustal belts in the Tartoq Group are very different from the other known belts in the Archaean block of SW Greenland. First of all they have experienced lower metamorphic conditions (greenschist facies versus amphibolite to granulite facies) and more importantly they consist almost exclusively of sedimentary lithologies rather than volcanic rocks. A shelf setting is thus a likely environment of deposition for the Tartoq Group supracrustal rocks, but further field observations and geochemistry is required to determine this with confidence.

The Tartoq metamorphic sequence: Using tourmaline to reconstruct its thermal and chemical history

Vincent van Hinsberg

The Tartoq group

The rocks of the Tartoq group in SW Greenland consist of a sequence of low-grade metamorphosed marine sediments, volcanoclastics and lavaflows. Lavaflows are present as small lenses up to massive sheets that are several meters in thickness, and are interlayered with mafic volcanoclastics. The latter have been metamorphosed to chlorite + quartz +/- fuchsite greenschists, and are characterised by a deformation-induced knobbly weathering. Carbonate veining is locally abundant in these volcanoclastics.

The sedimentary sequences are varied in appearance and composition. In the NW Nuuluk block, poorly consolidated sand channels are present in slate, and this sequence is itself contained within mafic greenschists, of probably volcanic origin. The greenschists show a bedding that is identical to that of the slates and interference between bedding and foliation leads to characteristic wedge-shaped weathering. Similar rocks, but of higher metamorphic grade are present in the Iterdlak block, with the appearance of biotite and an as-of-yet unidentified black porphyroblast phase. In the central part of the Nuuluk block, a thick sequence of meta-sediments is present, consisting, from west to east, of several alternating, meter-wide schist units grading from mafic greenschist to grey slates, followed by a several meter wide ridge of sulphide-rich rocks. These latter rocks are thinly bedded and contain abundant pyrite + pyrrhotite. The overall appearance of these rocks is that of a banded iron formation (Fig. 1), and abundant Fe-oxide grains oriented parallel to the bedding have indeed been observed in thinsection. Other sedimentary deposits in this part of the Nuuluk block include carbonate layers, banded quartzites and cm-thick graded tuff or ash layers.

At several locations, alteration zones are present within this sequence. These consist of white bands grading outward into the enclosing green schist and with a core that commonly shows malachite staining. No sulphides were recognised in these alteration zones, but these were present in more extensively stained faults.

Tartoq tourmaline

The initial part of this study has focused on tourmaline in these rocks and the information that can be derived from their composition on the conditions during its formation.

Tourmaline is present as small, up to mm-sized grains, mostly idiomorphic in shape and enclosed in the mica foliation. All tourmaline grains display zoning, both growth zoning and sector zoning. Colour is variable and correlates with the host rock bulk composition. In fuchsite-bearing mafic compositions, tourmaline has blue rims and green cores, whereas in more Fe-rich rock compositions, cores are bluish green and rims brown.

Two tourmaline types are present in these rocks. The first type consists of isolated grains that are commonly rounded or even fractured and form augen in the foliation. These grains appear to detrital. In all cases they are overgrown by a thin rim of metamorphic tourmaline that is in textural equilibrium with the metamorphic mineralogy and shows polar

growth and sector zoning (Fig. 2). The second type consists of mostly idiomorphic grains of tourmaline, present as both isolated grains and concentrated along specific foliation planes. The grains appear to be in equilibrium with the metamorphic mineralogy. Size, shape and abundance of these tourmaline grains are constant across bulk compositional contrasts, but colour varies. This suggests that tourmaline is related to later influx of B, as these host rocks should have strongly different initial B-contents.

Applying tourmaline inter-sector thermometry (van Hinsberg and Schumacher 2007) to the overgrowth rims on the detrital grains constrains the temperature of their formation to 370 +/- 45 ºC. This temperature is in excellent agreement with that obtained from Ca-Na exchange between tourmaline and plagioclase, which gives 375 +/- 20 ºC using the relation presented in van Hinsberg and Schumacher (2009). Preliminary data for the second type of tourmaline suggest higher temperatures of formation at 500 ºC, based on inter-sector thermometry. These tourmalines are also characteristically enriched in F, and depleted in the alkalis, compared to the metamorphic tourmaline grains. However, more work is needed to confirm that these differences are not related to variations in bulk-rock composition.

Pyrite and pyrrhotite replace the original iron-oxide mineralogy of the banded iron formation rocks and it appears that the second tourmaline generation accompanies this replacement. If this were confirmed, this would indicate that this replacement took place at the relatively high temperature of 500 ºC from a fluid bearing both S and B, and will allow tourmaline composition to be used to place constraints on the trace element composition of the fluid that induced this replacement.

References

van Hinsberg, V.J. and Schumacher, J.C. (2007) Intersector element partitioning in tourmaline: a potentially powerful single crystal thermometer. Contributions to Mineralogy and Petrology 153, 289-301.

van Hinsberg, V.J. and Schumacher, J.C. (2009) The geothermobarometric potential of tourmaline, based on experimental and natural data. American Mineralogist 94, 761-770.

Figure 1. *Thinly bedded sulphide-rich rocks in the central part of the Nuuluk block.*

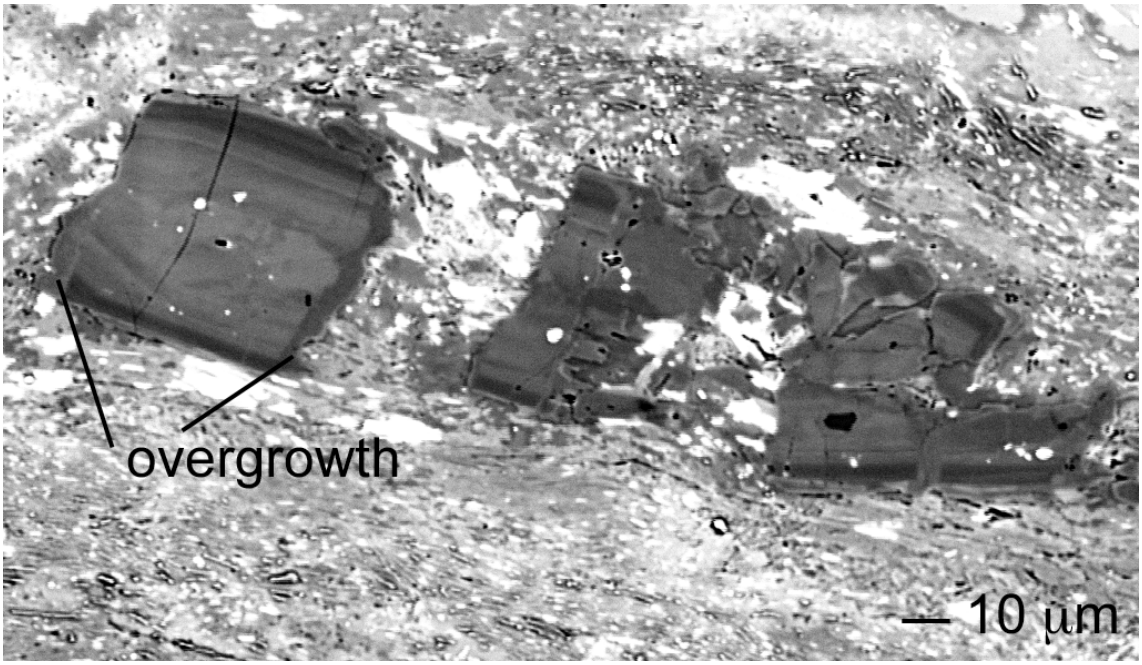

Figure 2. *Back-scattered electron image of a fractured zoned detrital tourmaline grain with metamorphic polar overgrowths.*